2022-04-20

Catalytic Light Crude Upgrading under Methane Environment

Li, Yimeng

UNIVERSITY OF CALGARY

Catalytic Light Crude Upgrading under Methane Environment

by

Yimeng Li

A THESIS

SUBMITTED TO THE FACULTY OF GRADUATE STUDIES

IN PARTIAL FULFILMENT OF THE REQUIREMENTS FOR THE

DEGREE OF MASTER OF SCIENCE

GRADUATE PROGRAM IN CHEMICAL ENGINEERING

CALGARY, ALBERTA

APRIL, 2022

Abstract

The catalytic upgrading of light crudes is a very important aspect of the petrochemical industry. In recent years, the desulfurization of marine fuels and the deoxygenation of biofuels attract more attention due to the implementation of IMO 2020 sulfur emission regulation and the increased demand for renewable fuels. In this thesis, the catalytic desulfurization of marine gas oil and marine diesel oil, as well as the catalytic deoxygenation of vegetable oil are both conducted under a methane environment, and using various catalyst supports doped with several metal species. Besides, some control experiments are also conducted under a nitrogen environment while the other reaction conditions remain the same. This research aims at fine performances of reducing sulfur and oxygen content within the light oils and oil quality improvement while yielding coke at a low level through methane-assisted catalysis. Catalysts are screened to gauge those with the best performances. As a result, the methane-assisted desulfurization and deoxygenation techniques are proved to be feasible and achieve promising performances of sulfur or oxygen content removal. The participation of methane during the upgrading processes not only promotes the desulfurization and deoxygenation performances but also improves the quality of the product oils, and reduces coke yields.

Acknowledgments

First and foremost, I would gratefully acknowledge the support provided by my extremely supportive supervisor, Dr. Hua Song, without whom I would not have been able to complete this research with the quality seen here. Dr. Hua Song's financial support has enabled me to study in Canada as a Chinese international student and provided me with a precious opportunity for graduate research. More importantly, the guidance and expertise that I obtained from Dr. Hua Song through my M.Sc. degree greatly helped the establishment of my research ability and laid the foundation for my possible Ph.D. studies.

Further acknowledgment is given to my group members for their substantial support and assistance in my research. These group members are Dr. Hao Xu, Dr. Zhaofei Li, Dr. Peng He, Dr. Aiguo Wang, Mr. Shijun Meng, and Mr. Jack Jarvis.

I would also gratefully acknowledge the financial support from KaraTechnologies Inc., Natural Sciences and Engineering Research Council of Canada (NSERC) through the Alliance Grant program (ALLRP/560812-2020) and collaborative research and development program (CRDPJ/53160718) and Alberta Innovates (G2020000355 and AI 2552). The technical support from Dr. CaiXia Hu of Synfuels China in the NMR study is greatly acknowledged.

In addition, I would like to thank Dr. Matthew Clark and Mr. Arthur de Vera for being there to answer my many questions.

Dedication

To

My dearest Mother and Father

Thank you for supporting me both financially and morally

throughout my academic career

My Wife

Thank you for taking care of me and encouraging me to progress

My friends and family

All my love

Table of Contents

List of Tables

List of Figures

Chapter One: Introduction

Catalytic desulfurization and deoxygenation processes are employed in oil refineries all over the world to produce oil products that are more environmentally friendly with lower sulfur content or more stable with lower oxygen content. Nowadays, the most widely used techniques for both processes are hydrodesulfurization (HDS) and hydrodeoxygenation (HDO) which are operated under a high-pressure hydrogen environment. Since the hydrogen is mostly obtained from the steam reforming process of methane, the capital and operational cost of hydrotreatment are enormous. This thesis shows the technical feasibility of utilizing methane as a direct hydrogen doner participating in the catalytic desulfurization and deoxygenation processes of various oil feedstocks at moderate temperatures and pressures.

1.1 Background of marine gas oil and marine diesel oil

In modern society, various types of light crude oil cannot be directly used as fuel in transportation or other human activities due to the conflicts between their properties and numerous industry regulations. For instance, according to the 2020 regulation made by the International Maritime Organization (IMO), the operating ships must use fuel with a sulfur content no larger than 0.5% m/m in any seas or oceans around the world. In some designated emission control areas (ECAs), the sulfur limit of marine fuels must be lower than 0.1% m/m [1]. The regulation greatly changed the global market of marine fuels, some types of light fuel oil with sulfur content below 0.5% replace the heavy fuel oil with much higher sulfur content (usually 2% - 3.5%) as the dominant force in the market share. Besides, as the overall price of marine fuel rises, the fuel with lower than 0.1% sulfur content but a relatively high price becomes more competitive. From February 2020 to August 2020, the very-low-sulfur fuel oil (VLSFO) with sulfur content between 0.1% and 0.5% such as marine diesel oil (MDO) and marine gas oil (MGO) had a global average

price of $367.5 per ton, while the low-sulfur marine gas oil (LSMGO) with sulfur content below 0.1% had an average price of $487.5 per ton globally in the same period. Meanwhile, the average price of VLSFO and LSMGO in the U.S is $384.5 per ton and $516.0 per ton [2]. Based on these data, a roughly $120 to $131.5 per ton extra profit can be obtained if a VLSFO can further reduce its sulfur content to lower than 0.1%, which provides a vast commercial penitential for the desulfurization process of VLSFO.

MGO and MDO as the typical VLSFO have been widely used since the 2020 IMO regulation was put into effect. MGO consists exclusively of distillates of crude oil and largely shares the same properties as standard heating oil. It has a transparent to light color, low density, as well as low viscosity at room temperature so that it can be easily pumped into the ship's engines at around 20 ^{o}C [3]. According to the ISO 8217:2017 fuel standard, MGO can be distinguished into several quality grades such as DMX, DMA, and DMZ. The maximum density at 15 ^{o}C, maximum sulfur content, minimum flashpoint, and the maximum acid number of these three grades are 890 kg/m^3, 1.00 wt%, 43 to 60 ^{o}C, and 0.5 mg KOH/g, respectively [4].

MDO represents the marine fuels that are made up of various blends of MGO and heavy fuel oil (HFO), but with very low HFO content. The oil refinery can directly control the different blending ratios of MDO. The properties of MDO are similar to diesel fuel, its color ranged from light brown to black due to the pollution of HFO, and it is also distinguished into two quality grades DMB and RMA 10 [5]. The maximum density at 15 ^{o}C, maximum sulfur content, minimum flashpoint, and the maximum acid number of DMB and RMA 10 are 900 to 920 kg/m^3, 1.50 to 3.5 wt%, 60 ^{o}C, 0.5 to 2.5 mg KOH/g, respectively [4].

1.2 Background of the hydrodesulfurization technologies

Hydrodesulfurization is the most commonly used technology in oil refineries for the

desulfurization of petroleum products which can efficiently remove sulfur from almost all kinds of distillates of crude oil including vacuum residue, heavy oil, middle distillates, and light oil. It is a key catalyst-driven process for the product streams [6]. HDS is considered one of the most essential steps in the production of cleaner end-products that removes around 2500 million metric tons of sulfur from crude oil per year globally [7]. The general hydrogen pressure of the HDS process is 5 to 160 bar, while the temperature ranges from 260 to 380 ^{o}C [8]. Various products can be yielded from different distillates streams such as light naphtha, kerosene, and low sulfur fuel oil (LSFO) which contains MGO and LSMGO [8]. The HDS reactions during the process can be classified as follows [8]:

Mercaptans:

$$RSH + H_2 \rightarrow RH + H_2S$$

Sulfides:

$$R_2S + 2H_2 \rightarrow 2RH + H_2S$$

Disulfides:

$$(RS)_2 + 3H_2 \rightarrow 2RH + 2H_2S$$

Thiophenes:

$$SCH{=}CHCH{=}CH + 4H_2 \rightarrow C_4H_{10} + H_2S$$

The typical catalysts for the HDS process are porous alumina support with a surface area of 200 to 300 m^2/g impregnated with combinations of cobalt (Co), nickel (Ni), molybdenum (Mo), and tungsten (W). Co-Mo/Al_2O_3 and Ni-Mo/Al_2O_3 are the most universally applied catalysts for HDS due to their good poisoning resistance [8]. During the past decades of optimizing the HDS

process, various reactors have been reported and applied to industrial HDS. An ebullated bed reactor achieves up to 90% sulfur removal dealing with heavy crudes with high asphaltene by using catalyst particles smaller than 1 mm [9]. A moving bed reactor has been designed to partially remove the contaminants whin the crude oil before it processing in the conventional fixed-bed reactors [10]. A multistage reactor using liquid-liquid extraction of sulfur species archives up to 99.5% sulfur reduction [11].

The major drawbacks of the HDS technique are the high operational cost due to the high H_2 pressure applied. In addition, since massive CO_2 is produced during H_2 production, the environmental problems caused by the HDS process are also severe.

1.3 Background of canola oil and the first-generation biodiesel

In the 21st century, with the shortage of fossil energy sources becoming severe globally, the development and usage of renewable energy sources such as biofuels have made huge progress. Biodiesel, one of the most widely used biofuels is primarily produced by processing vegetable oils such as canola oil, soybean oil, grape seed oil, and other seed oils. In 2019, the world's total daily production of biofuels was 1790 thousand barrels, while biodiesel reached 723 thousand barrels per day of production [12]. Europe has the highest share of 34.2% of global biodiesel production, followed by the Asia Pacific, the United States, and Brazil which count for 33.5%, 14.1%, and 13.2%, respectively [12].

Canola oil as one of the most common feedstocks in biodiesel production mainly consists of various triglycerides which are the ester of one molecule of glycerol and three molecules of fatty acids. 94.4% to 99.1% of the total lipid within canola oil is constituted by triglycerides [13]. The majority of fatty acids in canola oil have 18 carbon atoms which are oleic acid, linoleic acid, linolenic acid, and stearic acid accounts for 60.1%, 20.1%, 9.1%, and 1.5% of the total fatty acids,

respectively. The relative density at 20 ^{o}C, viscosity at 20 ^{o}C, flashpoint, and specific heat at 20 ^{o}C of are 0.914 to 0.917 g/cm^3, 78.2 mm^2/sec, 275 to 290 ^{o}C, and 1.910 to 1.916 J/g, respectively [13]. It is capable of directly using canola oil and other types of vegetable oil in diesel engines, but several abnormal phenomena occur during the operations mainly due to the injection, atomization, and combustion characteristics of vegetable oils being different from those of traditional diesel fuels. For example, the high viscosity of vegetable oils leads to poor fuel atomization during the injection. The high flash point leads to more deposit formation and carbonization of injector tips. Poor cold engine start-up, misfire, and ignition delay occur due to the combination of high viscosity and low volatility of vegetable oils [14]. Therefore, it is necessary to convert vegetable oil into other types of diesel-like biofuels to achieve higher efficiency and better performances during the operation of diesel engines.

The biodiesel in the current stage can be generally divided into first-generation biodiesel and second-generation biodiesel. The first-generation biodiesel, also known as fatty acid methyl ester (FAME) is produced by catalytic transesterification reaction of triglycerides as shown in Fig.1.1 [15]. In this reaction, triglycerides react with methanol by using homogeneous base catalysts or heterogeneous catalysts to yield FAME and glycerin. NaOH and KOH have been proven to be the most suitable homogeneous base catalysts for transesterification reactions and have been widely applied in industry. According to the transesterification protocol shown in Fig.1.2 [16], firstly, methanol is reacted with vegetable oils in the presence of KOH. Then, the crude biodiesel and the crude glycerin as the main products are separated when the reaction is completed. At last, the glycerin is refined for further use, while the crude biodiesel is also refined and separated with methanol which is reused in the cycle [16]. However, several drawbacks such as producing plenty of wastewater, producing low-quality glycerol, corrosivity, and hard purifying of the biodiesel product are quite obvious when applying these catalysts [17–20]. The homogeneous catalysts such

as CaO-based catalysts, lithium-based catalysts, KOH supported on alumina, NaY zeolite, mordenite, bentonite, and MGO not only show excellent catalytic activity in the production of biodiesel but also being less corrosive, more environmentally friendly, safer, cheaper, easier to be regenerated and reused [17,21–29]. In general, the transesterification process is one of the most widely available technologies for industrial biodiesel production. It solves the high viscosity problem of vegetable oil or animal fat in a very efficient and economical way due to its low cost, high conversion efficiency, and simplicity [30].

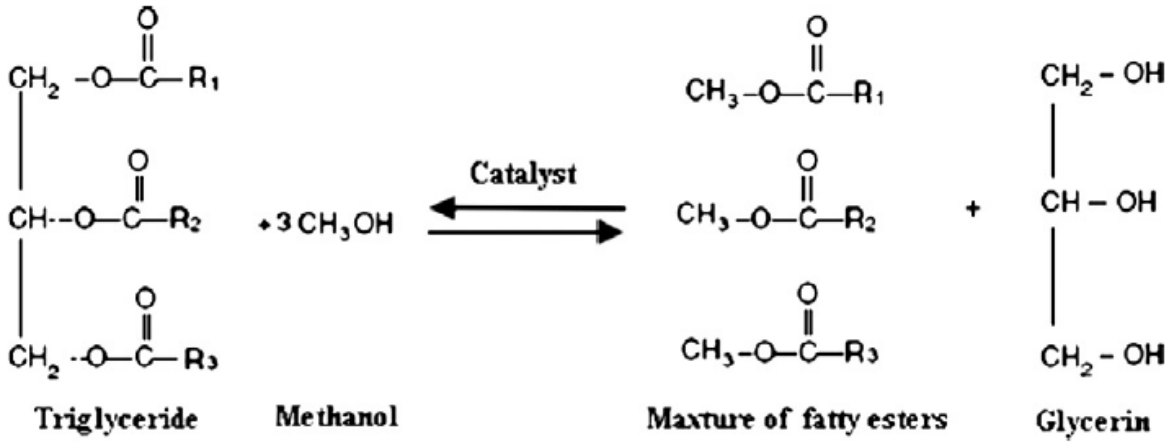

Fig. 1.1 Transesterification of triglycerides to yield fatty acid alkyl esters (biodiesel), reproduced with permission from Elsevier [15]

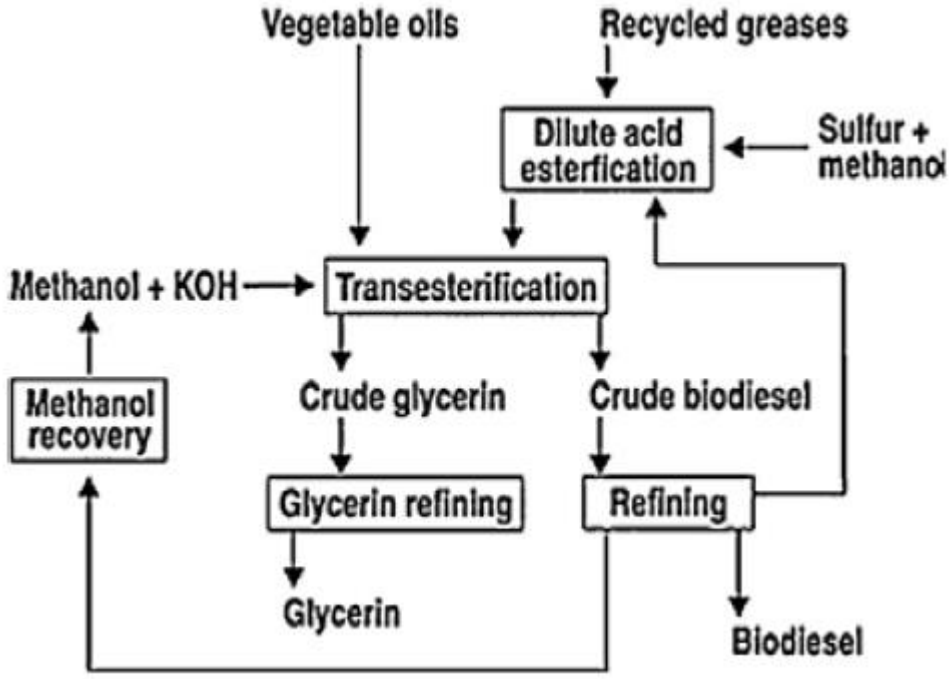

Fig. 1.2 Basic transesterification protocol, reproduced with permission from Elsevier [16]

1.4 Background of hydrodeoxygenation technologies

As mentioned, the transesterification reaction achieves the conversion from vegetable oil or animal fats to FAME which partially relieves the energy shortage. However, several problems with first-generation biodiesel are severe and inevitable due to its chemical properties. For example, its low cetane numbers and lubricity can cause engine corrosion, its high oxygen content and hydrocarbon evaporative emission lead to low stability within the combustion engines [31]. Other drawbacks such as poor cold flow properties, poor storage stability, low heating values, and high nitrogen oxides (NO_x) emissions make FAME less compatible with traditional diesel engines [32]. Therefore, developing the next generation, more advanced biodiesel becomes a major trend in the current biodiesel industry.

The second-generation biodiesel which has higher quality and stability than FAME is mainly

produced via the hydrodeoxygenation (HDO) process. The as-prepared biodiesel with very low oxygen, sulfur, and nitrogen content, high linear hydrocarbon content, excellent physical and chemical properties such as high cetane number, great cold flow properties, high heating value, and good storage stability can be fully compatible with fossil fuels for diesel engine usage [33]. A basic reaction scheme for HDO of triglycerides is shown in Fig. 1.4 [34]. At first, the hydrogenation reaction saturates the unsaturated fatty acid backbone of triglycerides. The saturated triglycerides then decompose into fatty acids under the effect of H_2. In this step, propane is produced as a by-product. A high concentration of fatty acids is observed in the initial stage of the HDO process due to the fast reaction of hydrogenation and decomposition of triglycerides [34]. Next, a reductive deoxygenation reaction of fatty acids occurs resulting in oxygen removal in the form of water and the fatty acids reduce to their respective fatty aldehydes. The deoxygenation of fatty aldehydes then proceeds directly through decarbonylation (DCO) reaction which produces CO and alkanes or via a dehydration process followed by hydrogenation reaction forming water and alkanes [34]. In addition, CO_2 formation is also observed during the HDO process mainly due to the water-gas shift reaction and possible decarboxylation process which are not mentioned in the reaction mechanism shown in Fig.1.4 [35].

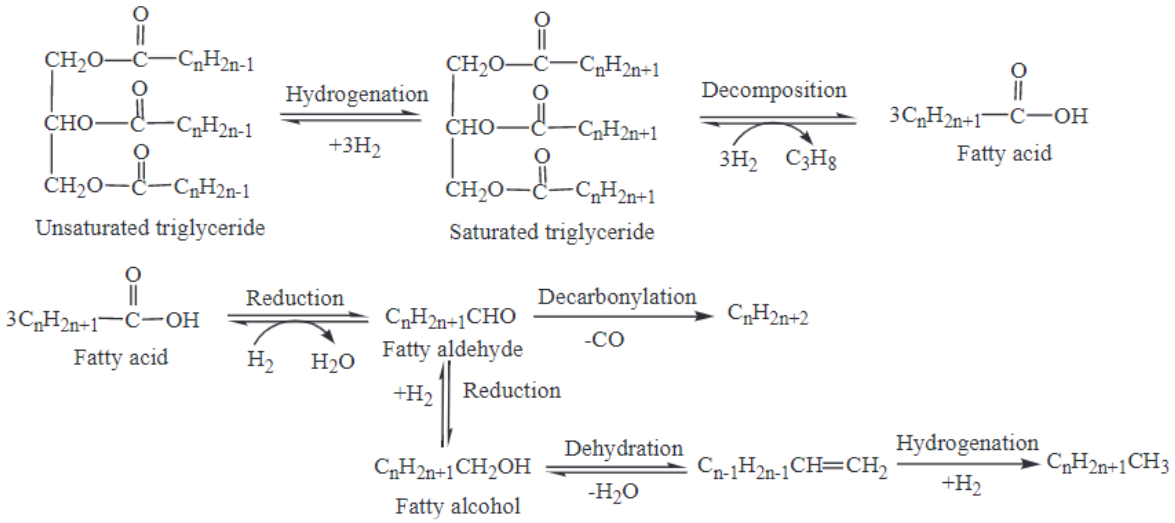

Fig.1.3 Reaction mechanism for HDO of triglycerides, reproduced with permission from Elsevier [34]

The production of second-generation biodiesel has been operating for more than a decade. For instance, a Finland-based company called Neste Oil developed a stand-alone process called NEXBTL that produces about 3 million tons of biodiesel [34]. This technology is a combination of HDO of vegetable oil and isomerization of linear alkanes to branched alkanes which can improve the cold flow properties of the products. The product biodiesel of NEXBTL exhibits a high heating value and high cetane number which are 44 MJ/kg and 84 to 99, respectively [34]. Another company called UOP honey well also developed a two-stage process for the production of second-generation biodiesel from fats, grease, and oils. Fig. 1.5 shows a schematic of the process [34]. In the first stage, the feedstocks undergo an HDO process in an adiabatic reactor obtaining diesel-ranged alkanes by immediately separating the CO_2, water, and valuable hydrocarbons. In the second stage, the diesel-ranged alkanes are converted to diesel-ranged branch alkanes via the hydroisomerization process to improve the cold flow properties of the end-product, while the excess H_2 is then recycled to both HDO and isomerization reactors. The final product of this technology also displays a high heating value of 44 MJ/kg and a high cetane number of 77 to 90 [34].

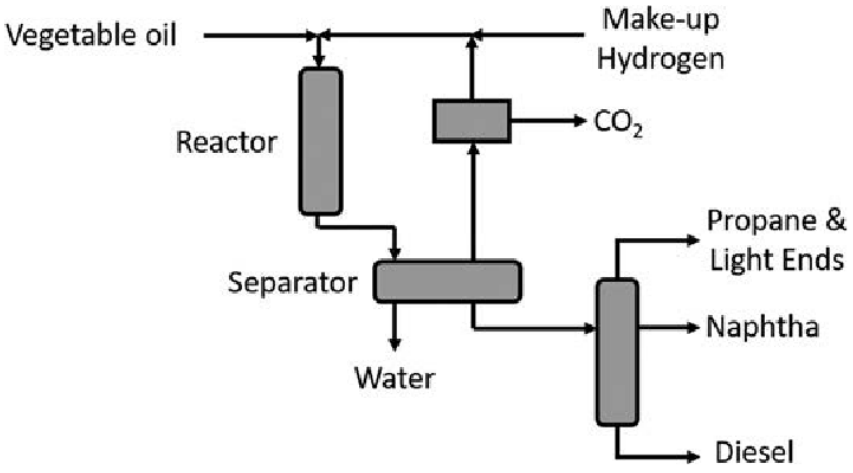

Fig. 1.4 Schematic representation of UOP eco-fining process, reproduced with permission from Elsevier [34]

1.5 Motivations for methane-assisted desulfurization and deoxygenation studies

Although the HDS and HDO provide promising sulfur and oxygen removal performances, some major drawbacks of these techniques considerably limited their industrial sustainable development.

Since hydrogen is not naturally reserved, around 75% of global hydrogen production relies on steam methane reforming (SMR) technology [36]. To apply the SMR process, a temperature as high as 800 ^{o}C, and a pressure ranging from 1.5 MPa to 3.0 MPa are required which causes the price of hydrogen to be much higher than the other commonly used feed gases in the petrochemical industry such as oxygen, nitrogen, and methane [37,38]. Moreover, the main reaction pathway in an SMR process is as follows [36]:

$$CH_4 + H_2O(g) \rightarrow CO + 3H_2$$

Since the reaction is highly endothermic which requires a large amount of heat to keep a constant temperature (i.e. 800 ^{o}C), so the SMR process produces a significant net amount of carbon dioxide along with hydrogen production. An average of 7 kg CO_2/kg H_2 is emitted from SMR facilities that contribute a large share of CO_2 emission within the petrochemical industry where 1.1 Gt of CO_2 emission has been reported in 2005, accounts for 16% of total industrial emission [36]. Therefore, using hydrogen for the desulfurization and deoxygenation processes not only leads to a high capital cost and operational cost but also results in severe environmental problems.

The serious defects of HDS and HDO motivate us to develop more advanced technologies to do the same jobs. Referring to the research background of our group, directly using methane as the

H donor for the desulfurization and deoxygenation process possesses a high research value and potential. These new technologies will significantly lower the capital and operational cost, as well as solve the CO_2 emission issue compared with the traditional HDS and HDO if they are commercialized. Thus, this thesis is aiming at investigating the feasibility of methane-assisted desulfurization and deoxygenation processes. More detailed experimental results will be shown in the following chapters.

1.6 Challenges of methane activation

Methane has the simplest molecular structure among hydrocarbons which presents a symmetrical tetrahedral configuration with four equivalent C-H bonds [39]. Due to the unusually strong C-H bonds among alkanes and other physical properties, the activation of methane requires more severe conditions (i.e. higher energy) than other commonly used gas feedstocks including hydrogen. For example, it is quite difficult to remove bound electrons of methane due to its extremely high ionization potential of up to 13.16 eV [39]. Moreover, methane demonstrates a low highest occupied molecular orbital (HOMO) energy level as well as a high lowest unoccupied molecular orbital (LUMO) energy level which makes the electron loss from HOMO and electron capture of LUMO hard to achieve [39]. Thus, both an adequate amount of energy supply and proper catalysts are necessary for methane activation [39],

1.7 Objectives

The primary objective of this research is to formulate the catalysts capable of removing sulfur content from marine gas oil and marine diesel oil, as well as removing oxygen content from canola oil to produce second-generation biodiesel under a methane environment at moderate temperatures and pressures. More detailed objectives are as follows:

1. Evaluate the properties of the feedstocks provided by industry or purchased from the market.

2. Select the feedstock with proper sulfur and oxygen content to make the experiment meaningful and promising.

3. Prepare a suitable reactor system to replicate the industrial processes at the lab scale.

4. Screen different catalyst formulations and analyze their performances by evaluating the properties of the products.

5. Evaluate the effect of methane by comparing methane-assisted reactions with control reactions conducted under a nitrogen environment.

6. Evaluate the fresh and spent catalysts to investigate the possible mechanism of the reactions.

1.8 Thesis organization

This thesis is organized into five chapters including two published journal pieces. I, Yimeng Li have conducted the majority of experiments and data analysis with assistance from my group members in terms of final submission and interpretation of results. These group members are Dr. Hao Xu, Dr. Zhaofei Li, Dr. Peng He, Mr. Shijun Meng, and Mr. Jack Jarvis. Dr. Hua Song, the principal investigator, provided technical assistance in all aspects of this work, providing advice and recommended steps. Dr. Caixia Hu was instrumental in assisting with NMR analysis.

Chapter 1 gives a brief introduction to marine gas oil, marine diesel oil, canola oil, first-generation biodiesel, second-generation biodiesel, hydrodesulfurization, and hydrodeoxygenation, also including the objectives and the organization of the thesis. Although an introduction is

provided, more detailed introductions are given in each chapter regarding the journals published.

Chapter 2 provides the details of the instruments that have been used and the experimental set-ups.

Chapter 3 investigates the feasibility of methane-assisted desulfurization of marine gas oil and marine diesel oil. This chapter is published in volume 289, article 119864 of "Fuel" as "*Catalytic desulfurization of marine gas oil and marine diesel oil under methane environment*".

Chapter 4 investigates the feasibility of methane-assisted deoxygenation of vegetable oil. This chapter is published in volume 311, article 122504 of "Fuel" as "*Catalytic methanotreating of vegetable oil: A pathway to Second-generation biodiesel*".

Chapter 5 demonstrates a conclusion to this work and delivers recommendations for future studies to be undertaken during my Ph.D. studies.

Chapter Two: Experimental Methods

2.1 Feedstock and chemicals

2.1.1 light oil feedstock

Marine gas oil and marine diesel oil provided by Kara technology Inc. are directly used as feedstocks for desulfurization experiments without any treatment.

Vegetable oils such as canola oil and soybean oil are purchased from supermarkets in Canada and directly used in the deoxygenation experiments without any treatment.

2.1.2 Chemicals

A mixed gas containing 10.000% molar of nitrogen and 90.000% molar of methane purchased from Air Liquide Canada Inc. is used as the feed gas for methane-assisted desulfurization and deoxygenation experiments. In addition, a pure nitrogen gas purchased from Air Liquide Canada Inc. with 99.999% of purity is used as the feed gas for the control experiments which are conducted under nitrogen environments.

2.2 Catalyst preparation

2.2.1 Preparation of catalyst supports

In general, all catalyst supports used in methane-assisted desulfurization and deoxygenation studies are homemade zeolite material and other inorganic support materials including alumina oxide and titanium silicate which are purchased from the industrial manufacturer and being used without any treatment. In chapters 3 and chapter 4, the homemade zeolite support, so-called UZSM-5 is synthesized using a hydrothermal technique via the following procedures: Firstly, aluminum nitrate nonahydrate ($Al(NO_3)_3{\cdot}9H_2O$) purchased from Alfa Aesar was added to a 1.0 M aqueous solution of tetrapropylammonium hydroxide (TPAOH) purchased from Sigma-Aldrich, followed

by stirring at room temperature until the dissolution of $Al(NO_3)_3 \cdot 9H_2O$ is completed. Secondly, Tetraethyl orthosilicate (TEOS) purchased from Sigma Aldrich was added dropwise under stirring to the solution as prepared above. Once the TEOS addition of TEOS is completed, the solution was then stirred at room temperature for around 1.5 h where supersaturation occurred. The resultant supersaturated gel was moved to an autoclave and started crystallization at 180 ^oC for 72 h. Upon the completion of the hydrothermal synthesis, the resultant pastes were recovered by vacuum filtration with multiple times washing using deionized water, followed by calcination in air at 550 ^oC and held for 4 h. The resultant power is denoted as UZSM-5 with an 80:1 SiO_2/Al_2O_3 ratio.

2.2.2 Metal loading of catalyst supports

Gallium, Molybdenum, and cerium were solely or in pairs loaded onto the UZSM-5, Al_2O_3, and TS-1 supports by using the incipient wetness impregnation (IWI) or wetness impregnation (WI) methods through the following procedures: Firstly, three metal salts gallium nitrate hydrate ($Ga(NO)_3 \cdot xH_2O$) purchased from Sigma-Aldrich and Alfa Aesar, ammonium molybdate tetrahydrate ($(NH_4)_6Mo_7O_{24} \cdot 4H_2O$) purchased from Alfa Aesar, and cerium nitrate hydrate ($Ce(NO)_3 \cdot 6H_2O$) purchased from Sigma-Aldrich were solely solved in an aqueous solution mixed with the catalyst supports, followed by drying in an oven at 92 ^oC or 110 ^oC overnight. The resultant powder or pellets was then calcined at 550 ^oC for 4 to 5 h in ambient air after each metal was loaded. The mass percentage of Ga, Mo, and Ce were 1%, 5%, and 5%, respectively.

2.3 Reactor system

A fixed-bed reactor shown in Fig. 2.1 was selected as the reactor system for both desulfurization and deoxygenation experiments. This system has three gas lines individually controlled by a calibrated mass flow controller with a controlled range of 5 to 100 mL/min which can be used to deliver gas feedstock. Liquid feedstock can be sent into the system through a high-

pressure metering pump with a rate of 0 to 10 mL/min. Catalyst powders or pellets with a volume of up to 10 mL can be held inside a vertically oriented reactor which can be heated by an electric furnace up to 600 ^{o}C and operated under a down-flow fixed-bed mode. The liquid product is condensed in a stainless-steel condenser attached to a benchtop chiller which can control the temperature of condensation. In chapter 4, a schematic of this reactor system is shown in Fig. 4.1.

Fig. 2.1 fixed-bed reactor used for methane-assisted desulfurization and deoxygenation studies

2.4 Characterizations

The characterizations of gas-phase products were accomplished by online gas chromatography (Agilent Micro-GC 490) which can identify and quantify the gas species in the inlet and outlet gases from the reactor system.

The characterizations of liquid-phase products were achieved through gas chromatography-mass spectrometry (GC-MS), elemental analysis, simulated distillation analysis, density measurement, total acid number measurement, inductively coupled plasma optical emission spectroscopy (ICP-OES), carbon-13 nuclear magnetic resonance spectroscopy (^{13}C NMR), and

proton nuclear magnetic resonance spectroscopy (^{1}H-NMR).

The characterizations of solid-phase products were accomplished by thermalgravimetric analysis (TGA) which mainly focuses on quantifying the coke formation on the surface of the spent catalysts.

The characterizations of fresh and spent catalysts were achieved through ammonia-temperature programmed desorption (NH_3-TPD), N_2 adsorption-desorption analysis, and X-ray diffraction (XRD).

The details of the characterization methods used in methane-assisted desulfurization and deoxygenation studies are shown in Chapters 3 and 4.

2.5 Performance evaluation

Under a fixed bed reactor mode, all experiments were carried out under similar conditions. Typically, the catalyst was loaded into the constant temperature section of the reactor. To control the position of the catalyst, ceramic balls were loaded above and below the catalyst bed. The reactor temperature was controlled by electric heating devices. To record the amount of oil intake, an electric scale was put under the raw material tank. The pressure of the reactor was maintained at a certain level with a methane flow. The methane/nitrogen gas flow rate was controlled and measured by a mass flow controller. After liquid-gas separation, the product oil entered the condenser. The weight change of the condenser after the collection was regarded as the amount of oil production. When the reaction was done, nitrogen was introduced to replace methane in the reactor system. After cooling, the reactor was detached, and the catalyst was discharged for the measurement of the coke generation rate.

The liquid and gas yields are calculated by the following equations:

$$\text{Liquid Yield} = \frac{\text{mass of liquid products}}{\text{mass of feed oil}} \times 100\%$$

$$\text{Gas Yield} = \frac{\text{mass of produced gas}}{\text{mass of feedstock}} \times 100\%$$

The coke formation rate is calculated by the following equation:

$$\text{Coke Formation Rate} = \frac{\text{mass of coke on used catalyst}}{\text{mass of catalyst} \times \text{rection time}} \times 100\%$$

The methane conversion is calculated by the following equation:

$$\text{Methane Conversion} = \left(1 - \frac{\text{mole of remaining methane after reaction}}{\text{mole of fed methane}}\right) \times 100\%$$

Chapter Three: Catalytic Desulfurization of Marine Gas Oil and Marine Diesel Oil under Methane Environment

This chapter is adapted from the following publication:

Yimeng Li, Peng He, Zhaofei Li, Hao Xu, Jack Jarvis, Shijun Meng, Hua Song. Catalytic desulfurization of marine gas oil and marine diesel oil under methane environment. Fuel 2021; 289: 119864. https://doi.org/10.1016/j.fuel.2020.119864.

3.1 Abstract

The desulfurization of marine gas oil (MGO) and marine diesel oil (MDO) is crucial for the bunker fuel industry due to the new regulation on SO_x emission imposed by the International Maritime Organization. The catalytic desulfurization of such feedstock is conducted under a methane environment in this study. Using a ZSM-5 with uniform cylindrical morphology (UZSM-5) as the catalyst support material, the over-cracking of oil molecules is inhibited. The incorporation of Ga and Mo enhances the activation of methane, aromatization of the feedstock, and conversion of sulfur-containing groups, particularly when marine diesel oil with a higher sulfur content is charged as the feed. Under the CH_4 environment, 58.8% sulfur content in the feedstock is converted compared with that of 42.8% under the N_2 environment when Ga-Mo/UZSM-5 is employed as the catalyst. The participation of methane not only improves the desulfurization performance but also suppresses coking and over-cracking of the feedstock as well as increasing the liquid product yield probably through methane incorporation into the product molecules.

3.2 Introduction

The latest regulations on sulfur emission made by the International Maritime Organization (IMO) have been put into effect since 1 January 2020. The limit of sulfur content in bunker fuels used on the ships within designated emission control areas (ECAs) remains at < 0.1% m/m, while the limit for the sulfur content outside ECAs is tightened to 0.50% m/m, reduced dramatically from 3.5% m/m as regulated in the previous IMO standard. It is estimated that sulfur oxide (SOx) will thus be reduced by around 8.5 million tons annually, counting for a 77% reduction in SOx emission from maritime activities globally [1]. The new regulation will directly benefit environmental protection and human health. However, it will also significantly impact the marine fuel industry due to the predictable highly increased fuel refining and upgrading cost. To meet the 0.50% m/m

sulfur content limit, high-sulfur fuel oil (HSFO) such as intermediate fuel oil (IFO) and heavy fuel oil (HFO), which used to be the most commonly used marine fuel, may continue to be used only if an exhaust gas cleaning system (EGCS) was installed on vessels. Otherwise, the fuel has to be switched to use very-low-sulfur fuel oil (VLSFO) such as marine diesel oil (MDO) with sulfur content below 0.5%. Furthermore, an even stricter sulfur limit < 0.10% m/m is applied inside ECAs, where the ship engines have to consume ultra-low-sulfur fuel oil (ULSFO) where low-sulfur marine gas oil (LSMGO) is the only feasible option at the current stage. Based on the projection model shown in the assessment of fuel oil availability report published by IMO, the global demand for classified marine fuels in 2020 was predicted as follows: The estimated annual bunker fuel demands of ULSFO, VLSFO, and HSFO are 33–48 million tons, 198–200 million tons and 14–38 million tons, respectively [40].

With the new regulations in place, it is predicted that VLSFO and ULSFO will be used to meet the major demand in the bunker fuel industry and occupy most of the market share. Between mid-February to early August in 2020, the global average bunker prices of VLSFO, LSMGO, and IFO380 are $367.5, $487.5, and $287.5 per ton, respectively, while the average bunker prices of VLSFO, LSMGO, and IFO380 in the US are $384.5, $516.0 and $354.5 per ton in the same period [2]. The price of the fuel is greatly affected and determined by its sulfur content, making it economically promising to upgrade the bunker fuel to achieve a reduced sulfur content.

Hydrodesulfurization is commonly practiced in the industry to break down the C-S bond under an H_2 environment and convert sulfur-containing species in the bunker fuel in the form of H_2S. However, this process has to consume hydrogen, which is not naturally available. In industry, more than 50% hydrogen is obtained through the steam reforming process of natural gas at high operating temperature (>800 ^oC) and pressure (1.5–3.0 MPa) [37,38]. The hydrodesulfurization is also

executed at high pressure (e.g. 13 MPa) as well, resulting in increased operating costs. Instead of using hydrogen, if natural gas can be directly used as the hydrogen source, the steam reforming process can be skipped, leading to a significant cost reduction in the desulfurization process. The utilization of methane, the principal component of natural gas, as an alternative hydrogen source has been explored in several systems such as heavy oil [41,42], paraffin [43], and biomass [44] with metal species such as Ga and Mo in the catalyst to activate methane. It is noticed that such a methanotreating process produces extra products with reduced CO_2 emission thanks to the incorporation of CH_4 into the product molecules, making the upgrading under methane even more economically favorable and environmentally friendly.

Compared with hydrogen, it is more challenging to activate methane, which is more inert due to its stable molecular structure and strong C–H bond with a bond energy of 413 kJ/mol. It is critical to developing a catalyst system to efficiently break the C–H bond before allowing methane to participate in the desulfurization process. In the present work, UZSM-5 is employed as the catalyst support to control the cracking of carbon chains for increased liquid product selectivity without sacrificing the C–H activation performance. We have screened the catalyst composition using a variety of metal species to modify the UZSM-5 support. The catalytic performance is evaluated in terms of liquid yield, sulfur content reduction, and product compositional analysis. The catalytic performance is first evaluated using MGO, which has more light fractions and thus benefits the compositional analysis, as the feedstock to screen the catalyst. Sulfur content, liquid yield, total acid number, density, simulated distillation analysis, compositional analysis of the light distillates, and NMR analysis of the liquid products are executed to unveil the reaction network during the desulfurization process. The desulfurization under methane is further explored using MDO, which has heavier fractions, a larger molecular weight, and higher sulfur content, as the feedstock to demonstrate the feasibility of this process. The effect of methane is evaluated by comparison of the

product properties with those obtained under the N_2 environment.

3.3 Experimental

3.3.1Feedstock and chemicals

A marine gas oil (MGO) and a marine diesel oil (MDO) sample were acquired from Kara Technologies Inc. Both samples were directly used as the feedstock without further treatment.

3.3.2 Catalyst synthesis

UZSM-5 was synthesized by hydrothermal technique. Al $(NO_3)_3 \cdot 9H_2O$ (98%, Alfa Aesar) was added to 1.0 M Tetrapropylammonium hydroxide (TPAOH, Sigma Aldrich) and stirred at room temperature until a clear solution was obtained. Tetraethyl orthosilicate (TEOS, Sigma Aldrich) was then added dropwise to the above solution whilst maintaining stirring. Upon completion of TEOS addition, the solution was left to stir until supersaturation after approximately 1 h. The resulting supersaturated gel was applied to a Teflon-lined autoclave and treated in a furnace at 180 ◦C for 72 h. Amounts were calculated to obtain a molar ratio of Al_2O_3:80SiO_2:21TPAOH:943H_2O in the gel. After the hydrothermal synthesis, the powder was recovered by vacuum filtration and washing with deionized (DI) water 3 times. The resultant pastes were then heated at 110 ^oC in the oven for 8 h and subsequently calcined in air at a rate of 5 ^oC/min, held at 300 ^oC for 30 min, ramped at the same rate again, finally ramped at the same rate to 550 ^oC and held for 4 h. The resultant powder is denoted UZSM-5 for the ZSM-5 with uniform particle size and compact cylindrical morphology [45]. Then, UZSM-5 support was extruded to get the shaped pellets with a diameter of 1.0 mm and a length of 5.0 mm.

The metal modified UZSM-5 catalysts were prepared by incipient wetness impregnation of UZSM-5 support with an aqueous solution of ammonium molybdate tetrahydrate

($(NH_4)_6Mo_7O_{24}\cdot 4H_2O$, 99%, Alfa Aesar) and/or gallium nitrate hydrate ($Ga(NO_3)_3\cdot H_2O$, Alfa Aesar), dried in the oven at 92 ^oC overnight, followed by calcination at 550 ^oC for 5 h in ambient air after each metal was loaded. The resultant catalysts were denoted as Ga/UZSM-5, Mo/UZSM-5, and Ga-Mo/UZSM-5. The mass percentages of Ga and Mo were 1% and 5%, respectively.

3.3.3 Catalytic performance evaluation

Four reactions with MGO as feedstock were conducted using a fixed bed reactor under a methane environment. The position of the catalyst bed is in the middle of the reactor tube, which is filled with quartz wool and glass beads at the top and the bottom section. The reactor was loaded with 5 g of catalyst pellets and feedstock passed the catalysts with a down-flow mode and there was no inert diluent. The reaction temperature was 400 ^oC, the reaction pressure was 30 bar, the inlet gas flow rate was 100 sccm and the feedstock pumping rate was 0.09 mL/min. 5 g of catalyst was loaded for each reaction with a reaction time on stream of 6 h. The catalyst employed for each run was UZSM-5, Ga/UZSM-5, Mo/ UZSM-5, and Ga-Mo/UZSM-5, respectively.

Another two reactions applied on the micro-fixed-bed reactor with MDO as feedstock were conducted under a methane and nitrogen environment. Both reactions were using Ga-Mo/UZSM-5 as the catalyst and other conditions were the same as those applied in MGO reactions.

3.3.4 Characterizations

To close the mass balance of each reaction, the gas yield was calculated using the summation of the average mass of generated gas every 30 min divided by the mass of consumed feedstock. The necessary data to determine gas yield and methane conversion was acquired through gas chromatography (Agilent Micro-GC 490), an inlet flowmeter within a fixed bed reactor system, and internal standard, i.e. N_2, was added to the feed gas. The liquid yield was the ratio between the

mass of the collected liquid oil and the mass of consumed feedstock.

Thermographic Analysis (TGA) signal along with the simultaneously collected Differential Scanning Calorimetry (DSC) signal fulfilled with a simultaneous thermal analyzer (PerkinElmer STA 6000) of the spent catalyst was acquired to calculate the coke yield as well as coke formation rate.

The density of the oil samples was measured using the Anton Paar DMA 4500 M density meter.

The total acid number (TAN) of the liquid sample produced from each run was measured using a Metrohm 848 Titrino Plus by averaging the results collected from at least three independent measurements.

Simulated distillation analysis of the feedstock and product oil samples was executed to compare the boiling point difference and estimate the average molecular weight, which is achieved by Agilent 8890 GC System equipped with an analysis software SimDis Expert developed by Separation Systems. Liquid nitrogen was used to realize the cryogenic GC analysis from -20 ^{o}C to 425 ^{o}C with a ramp rate of 10 ^{o}C/min. The boiling curves were calibrated using the reference sample SD-SS3E-05 supplied from Separation Systems. The average molecular weight of the feedstock and products were calculated using these simulated distillation curves.

The sulfur content was measured by a Thermo Scientific iCAP 7000 series ICP-OES spectrometer. Each sample was diluted into three different concentrations and measured at two different characteristic wavelengths to get reliable results.

The ^{13}C NMR experiments were conducted at 9.4 T ($\nu_0(^{13}C)$ = 100.6 MHz) on a BRUKER AVANCE III 400 spectrometer with a BBFO 5 mm probe. ^{13}C NMR chemical shifts were

referenced to $CDCl_3$ at 77.26 ppm. A spectral width of 24 kHz and a zgig 30 pulse with a delay of 2 s were used to acquire 1024 scans per spectrum. The NMR samples in the tubes are prepared by mixing 0.1 mg sample, 0.1 mg $Cr(acac)_3$, and 0.5 mL $CDCl_3$.

Ammonia-temperature programmed desorption (NH_3-TPD) was performed to determine the surface acidity of zeolite catalysts on a chemisorption analyzer (Finesorb-3010). Typically, 0.2 g catalyst was put into a U-type quartz tube and both ends were filled with quartz wool. To remove the adsorbed impurities, temperature-programmed oxidation (TPO) test was first performed, in which the tube was heated up to 600 ^oC and held for 30 min with a ramp rate of 20 $^oC\ min^{-1}$ under 5% O_2/He gas flow (flow rate 30 sccm). Then, the system was cooled down to 120 ^oC and ammonia adsorption was conducted by feeding 10% NH_3/He for 30 min (flow rate 25 sccm). Next, the physisorbed ammonia was flushed out by He gas flow for 30 min (flow rate 30 sccm). Finally, the desorption of ammonia was carried out from 120 ^oC to 800 ^oC with a ramping rate of 20 $^oC\ min^{-1}$ and held at 800 ^oC for 10 min. The desorbed ammonia was monitored by a thermal conductivity detector (TCD) and the amount was quantified by peak integration of the corresponding calibrated TCD signal.

N_2 adsorption-desorption analysis of catalysts was carried out on ASAP 2020 Plus surface area and porosimeter system (Micromeritics). The sample was first degassed at 350 ^oC for 4 h with a temperature ramping rate of 10 $^oC\ min^{-1}$ and a vacuum level of 20 μmHg. Then the analysis was performed in liquid nitrogen to get a 56-point adsorption-desorption isotherm. The total surface area was calculated by the BET method and the total pore volume was calculated at 0.995 relative pressure.

3.4 Results and discussion

3.4.1 Upgrading of marine gas oil (MGO)

Our previous studies have proved that the methanotreating approach was successful for a wide range of feeds including bitumen, asphaltene, heavy crudes, naphtha, and bio-crudes [46–51]. A series of metal-modified ZSM-5 catalysts with controlled acidity and metal loading types have been developed to upgrade different feedstocks under a methane environment. Different metal species may exhibit different adsorption and activation capacity toward different molecules and their functional groups. The careful tuning of the metal species loaded to the zeolite support is required to optimize the upgrading performance in terms of varied feeds. The first feedstock used in the desulfurization study is MGO because there are more light fractions in MGO than MDO. This feature would benefit the compositional analysis using GC-MS, which cannot accurately determine the composition of very heavy fractions, to grasp a better understanding of the desulfurization process. Therefore, we have compared the performance of catalysts with different metal loading conditions using marine gas oil with 0.2 wt% sulfur as the feedstock.

A challenge faced by the desulfurization process is the over-cracking of carbon chains while breaking the C–S bonds in the MGO molecules, resulting in a low liquid product yield. In our previous study, UZSM-5 has demonstrated suppressed carbon chain cracking capacity and thus increased liquid product selectivity without sacrificing the C–H activation performance [45,52]. The synthesized UZSM-5 has a rather high silica to alumina molar ratio of 80:1 and a low acid site concentration [53], making it effective in preserving the carbon chain structure during catalytic desulfurization. As shown in Table 3.1, when UZSM-5 without metal loading is employed as the catalyst, 0.03% of gas yield and 97.5% of liquid yield indicate that cracking barely occurs during the reaction. Since zeolite with MFI structure is widely used in fluid catalytic cracking (FCC) process with an operating temperature of around 500 ^{o}C, the temperature at 400 ^{o}C is not high enough to trigger the formation of carbenium ions. However, sulfur content is reduced from 1988 to 1404 ppm after the reaction (Table 3.2). This phenomenon indicates that the removal of sulfur-

containing moieties is probably due to the adsorption of the sulfur atoms to the acidic sites in the zeolite framework, as is evidenced by the trivial coke yield. Meanwhile, the methane conversion is nearly 0 due to the fact that CH_4 cannot be activated with a pure zeolite structure, which might be enhanced by the loading of active metal sites.

Table 3.1 Mass balance results of MGO desulfurization reactions using different catalysts

Catalyst	Gas yield/%	Liquid yield/%	Coke yield/%	Coke formation rate/h^{-1}	Overall yield/%	Methane conv./%
UZSM-5	0.03	97.5	0.63	0.006	98.2	0.03
Ga/UZSM-5	1.62	95.4	0.93	0.008	98.0	0.23
Mo/UZSM-5	3.10	91.7	1.35	0.012	96.2	0.27
Ga-Mo/UZSM-5	6.01	91.3	1.31	0.012	98.6	0.56

Ga has been reported as an effective component in methane activation [54]. Therefore, Ga modified UZSM-5 (Ga/UZSM-5) is employed in this work to upgrade MGO under a methane environment. The presence of Ga in the catalyst enhances the desulfurization activity of the catalyst by lowering the sulfur content in the product to 1267 ppm (Table 3.2), while the liquid product yield remains at a high level of 95.4%. Mo doped catalysts are not only employed in methane activation catalysts [41,55,56] but also often used in desulfurization catalyst systems [57,58] since the Mo site can be used as anchor sites for sulfur atoms. Therefore, Mo is also considered a promising metal candidate for the desulfurization of MGO in the present work. When Mo/UZSM-5 is employed as the catalyst in the reaction, the sulfur content of the product is further reduced to 1156 ppm (Table 3.2). It is also worth noting that the total acid number (TAN) of the product is decreased to 0.02 mg KOH/g from 0.08 mg KOH/g of the feedstock, equivalent to a 75% reduction of the acid groups in feedstock molecules, which may be closely related to the conversion of S containing groups. The liquid product yield is 91.7%, slightly lower than that from Ga/UZSM-5, indicating that the cracking of diesel molecules becomes more significant.

Table 3.2 Characterization results of MGO and its products

Catalyst	Density at 15.6 °C/(g/mL)	TAN/(mg KOH/g)	Sulfur content/ppm	Desulfurization percentage/%	Average molecular weight/(g/mol)
/	0.8524	0.08	1988	/	318
UZSM-5	0.8479	0.08	1404	29.4	305
Ga/UZSM-5	0.8358	0.07	1267	36.3	286
Mo/UZSM-5	0.8395	0.02	1156	41.9	284
GaMo/UZSM-5	0.8430	0.02	925	53.5	275

To combine the methane activation and sulfur removal functions of these metal species, Ga-Mo/UZSM-5 catalyst is prepared by the co-precipitation method. A more outstanding desulfurization activity is witnessed over the Ga-Mo/UZSM-5 catalyst. The sulfur content is decreased to as low as 925 ppm (Table 3.2), suggesting a synergistic effect of the Ga and Mo components in the desulfurization process. Along with the sulfur content, the density of the products is also reduced after the reactions. Methane activation and desulfurization appear to happen simultaneously on the surface of the catalyst. The sulfur species might be adsorbed on the Mo sites while the adjacent Ga sites would catalyze the CH_4 molecules to form H and CH_{4-x} moieties. Those species can help to form H_2S with those adsorbed sulfur species and are released into the gas phase leading to the creation of sulfur vacancies surrounding Mo atoms. Therefore, the overall desulfurization ability is greatly enhanced by using this catalyst.

The simulated distillation curves (Fig. 3.1) of the MGO feedstock and the products are obtained to better understand the reaction process. The average molecular weight (AMW) of the samples is tabulated in Table 3.2. It is observed that the feedstock has the highest boiling point distribution and the highest AMW of 318.3 g/mol. After the reaction over UZSM-5, the distillation curve slightly moves towards the low-temperature region, i.e., more diesel fractions are distilled at a given temperature, indicating a lowered boiling point of the product matrix. The average molecular

weight is also reduced to 304.7 g/mol, suggesting the cracking and the removal of S atoms from the product molecules during the reaction. When Ga/UZSM-5 and Mo/UZSM-5 are used to catalyze the reaction, the distillation curves further move to lower temperature regions and average molecular weight values are reduced to 286.3 and 283.8 g/mol, respectively. When Ga-Mo/UZSM-5 is employed as the catalyst, the distillation curve is above those obtained from other conditions and the average molecular weight is only 275.1 g/mol. These phenomena show that the product molecules become lighter upon the desulfurization process over Ga-Mo/UZSM-5.

The density of the MGO feedstock is 0.8524 g/cm^3 at 15.6 ℃, which is reduced to 0.8358, 0.8395, and 0.8430 g/cm^3 after the reaction over Ga/UZSM-5, Mo/UZSM-5, and Ga-Mo/UZSM-5, respectively. The sulfur-containing groups would increase the polarity of the molecules, which is related to the dipole-dipole force and the induction force between the molecules. As the sulfur-containing groups are converted, the Van der Waals interaction between the product molecules via these groups may be suppressed. As a consequence, the density of the product is significantly reduced after the reaction.

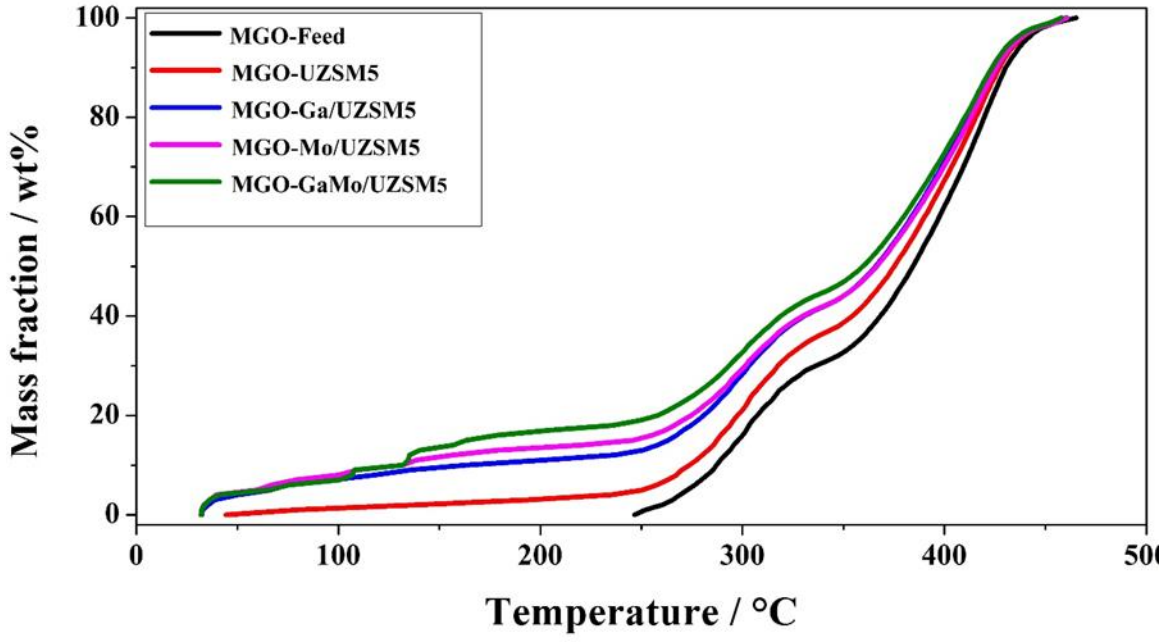

Fig. 3.1 Simulated distillation analysis curves of MGO and its products.

When comparing the density values of product oil after the reaction using Ga/UZSM-5, Mo/UZSM-5, and Ga-Mo/UZSM-5 as the catalyst, it is interesting to find that the density values follow the order of Ga/UZSM-5 < Mo/UZSM-5 < Ga-Mo/UZSM-5. However, the product from Ga-Mo/ UZSM-5 demonstrates the lowest S content and boiling point, while that from Ga/UZSM-5 has the highest ones. To better understand this phenomenon, we have conducted a more thorough analysis of the products using GC–MS. Because of the high boiling points of the heavy fractions in the product, we can only accurately quantify the compounds with boiling points below 250 ^{o}C, while heavier compounds cannot be separated by the GC column. However, we can still get some hint of the aromatization process taking place during the reaction by determining the selectivity of aromatic product molecules including benzene, toluene, ethylbenzene, and xylenes (BTEX). After the reaction over Ga- Mo/UZSM-5, the selectivity of aromatics is as high as 75.2% among the product molecules with boiling points below 250 ^{o}C (Table 3.3). The selectivity of BTEX is as high as 49.6%, which makes the upgrading more profitable since BTEX are valuable feedstocks in petrochemical production [59]. Notably, the increase of the BETX fraction could result in a significant increment of soot present in exhaust gases after the combustion. When Ga/UZSM-5 and Mo/UZSM-5 are used as the catalyst, the aromatic product selectivity is 14.2% and 50.6%, respectively. On the other hand, a negligible amount of BTEX is observed in the feedstock and the product obtained from the reaction using UZSM-5 as the catalysts. Besides the light distillates, we have acquired ^{13}C NMR spectra of the feedstock and product samples to evaluate the aromatization of all the fractions in the sample. The ^{13}C peak area assigned to carbons atoms in phenyl rings and due to paraffin and substitution groups is tabulated in Table 3.4. 13.2% of carbon atoms in the product obtained over Ga-Mo/UZSM-5 are attributed to phenyl rings, while only 8.6% and 8.9% of carbon atoms are in phenyl rings when Ga/UZSM-5 and Mo/UZSM-5 are employed. A

significantly improved aromatization is witnessed with Ga-Mo/UZSM-5 as the catalyst, which is in line with the compositional analysis results from GC–MS analysis. These results suggest that the aromatization process is more significant when Ga-Mo/UZSM-5 is the catalyst. The π-interaction between the phenyl rings enhances the interaction between the aromatic molecules, resulting in increased density of the product matrix. Therefore, the highest density of product obtained over Ga-Mo/UZSM-5 is observed along with the lowest distillation temperature and sulfur content.

Table 3.3 Aromatics selectivity of the MGO upgrading products (distillates < 250 °C)

Catalyst	Benzene /wt%	Toluene /wt%	Ethylbenzene /wt%	Xylene /wt%	Aromatics/ wt%
UZSM-5	0	0	0	0	0
Ga/UZSM-5	0	6.2	0	8.0	14.2
Mo/UZSM-5	0	11.1	3.9	18.3	50.6
Ga-Mo/UZSM-5	2.7	16.5	4.8	25.6	75.2

Table 3.4 ^{13}C NMR peak area percentages of MGO and the products assigned to carbons in phenyl rings, paraffin, and the substitution groups

Catalyst	Phenyl ring/%	Paraffin and substitution group/%
-	0	100
UZSM-5	0	100
Ga/UZSM-5	8.6	91.4
Mo/UZSM-5	8.9	91.1
Ga-Mo/UZSM-5	13.2	86.8

These phenomena show the promising desulfurization activity of these catalysts, particularly when both Ga and Mo are employed to modify UZSM-5. The cracking of the MGO molecules is

not severe with liquid product yields above 90% after the reactions. As desulfurization takes place, the conversion of sulfur-containing groups results in the reduction of TAN as well as the dipolar interaction. The MGO molecules are converted to smaller molecules with fewer sulfur-containing groups as the reaction proceeds. The sulfur content, boiling point, average molecular weight, and density of the product are decreased as a consequence. Besides the reduction of sulfur content, the aromatization process of the light fraction molecules leads to a considerable amount of BTEX products.

3.4.2 Upgrading of marine diesel oil (MDO)

Encouraged by these promising results during the desulfurization of MGO under a methane environment, we continue to explore the feasibility of this method in the upgrading of MDO, a blended fuel oil consisting of MGO as the major component and a very small portion of heavy fuel oil (HFO) with a higher sulfur content of 2153 ppm (Table 3.6). When Ga-Mo/ UZSM-5 is employed as the catalyst, the sulfur content of the product is reduced to 887 ppm, equivalent to a 58.8% sulfur content reduction, which is more dramatic compared with the desulfurization performance using MGO as the feedstock.

Table 3.5 Mass balance results of MDO desulfurization reactions using methane and nitrogen as feed gases

Catalyst	Feed gas	Gas yield /wt%	Liquid yield/wt%	Coke yield/wt%	Coke formation rate/h^{-1}	Overall yield/wt%	Methane conv./%
Ga-Mo/UZSM-5	CH_4	2.56	96.1	1.20	0.011	99.86	1.07
Ga-Mo/UZSM-5	N_2	2.82	95.4	1.34	0.012	99.57	-

It is also worth noting that methane participation is more remarkable under this condition, evidenced by a much larger methane conversion of 1.07% compared with 0.56% when MGO is the

feedstock. The TAN is decreased to 0.03 mg KOH/g from 0.24 mg KOH/g of the MDO feedstock along with the removal of S atoms. In addition, the liquid yield of the MDO reaction is higher than the MGO reaction with the same conditions, implying that more methane might be activated and incorporated into the products. Both the gas and coke yields are lowered compared with those derived from the MGO counterpart due to the suppression of over-cracking by the participation of more prominent methane engagement, leading to a higher liquid yield of 96.1% (Table 3.5). These phenomena indicate that the catalytic desulfurization under methane is even more feasible using MDO as the feedstock.

Table 3.6 Characterization results of MDO and its products

Sample	Density at 15.6 ℃/(g/mL)	TAN/(mg KOH/g)	Sulfur content/ppm	Desulfurization percentage/%	Average molecular weight/(g/mol)
MDO-Feed	0.85239	0.24	2153	0	375
MDO-CH_4	0.84176	0.03	887	58.8	281
MDO- N_2	0.83456	0.05	1231	42.8	269

To verify the contribution of the activated methane molecules in the desulfurization process, the control experiment with Ga-Mo/UZSM-5 catalyst under N_2 was carried out. The sulfur content is 1231 ppm in the product oil, much higher than that obtained under the CH_4 environment, i.e., 887 ppm (Table 3.6). The liquid product yield is 95.4%, lower than that obtained under the CH_4 environment, i.e., 96.1% (Table 3.5), while the gas yield is higher than the CH4 environment counterpart. These phenomena show that the participation of methane in the desulfurization process not only enhances the removal of S species but also improves liquid product selectivity. By comparing the simulated distillation curves of the MDO feedstock and the product oil samples obtained under the N_2 and CH_4 environment (Fig. 3.2), it is clear that the boiling point decreased after the upgrading. The average molecular weight decreased from 375 to 268 and 281 g/mol,

respectively (Table 3.6). It is noticed that the distillation temperature, average molecular weight, and density of the product obtained under the CH_4 environment are higher, suggesting the incorporation of methane into the liquid product molecules and the suppressed over-cracking of MDO molecules under the methane environment. These phenomena demonstrate the significance of methane participation in desulfurization in terms of improved conversion of sulfur atoms and increased liquid product yield.

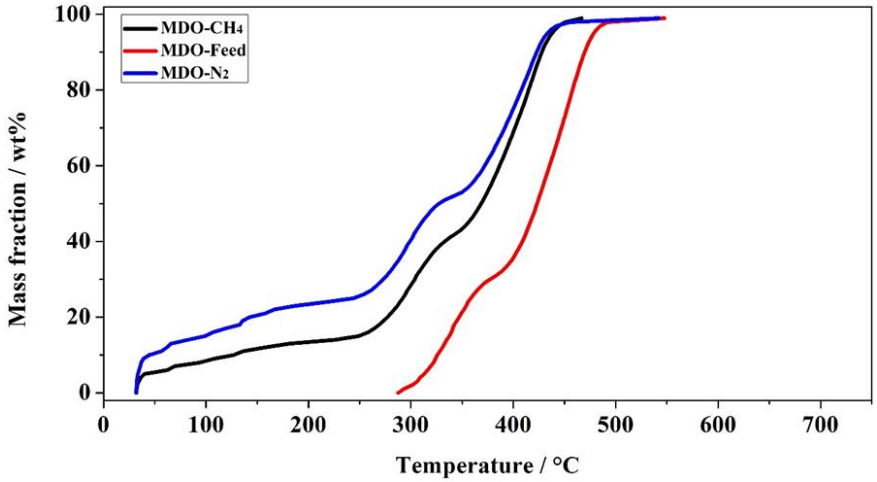

Fig. 3.2 Simulated distillation analysis curves of MDO and its products

3.4.3 Physicochemical properties of the catalysts

To better understand the physicochemical properties of the most promising catalyst, the porosity properties of UZSM-5 and Ga-Mo/ UZSM-5 were studied as shown in Table 3.7. It is noted that the shaped UZSM-5 support has a typical surface area and pore volume for an MFI-type zeolite structure. The loading of Ga and Mo results in slightly lower surface area and pore volume. However, the spent catalyst has a clear decrease in both the surface area and pore volume due to the formation of coke during the reaction, which is about 1.2% after 6 h (Table 3.5). The decrease of the surface area is about 22%, while the decrease of the pore volume is about 53%, implying that the majority of coke species existed at the mesoporous interstices between the zeolite particles.

Table 3.7 Porosity properties of UZSM-5 and Ga-Mo/UZSM-5 catalysts

Sample	BET surface area/(m^2/g)	Total pore volume/(ml/g)
UZSM-5	321	0.258
Ga-Mo/UZSM-5	287	0.224
Spent Ga-Mo/UZSM-5	224	0.105

The NH_3-TPD study of UZSM-5 and Ga-Mo/UZSM-5 is carried out to better understand the effect of metal loading on the catalysts in terms of acidity. The NH_3 desorption peaks of both samples appear below 250 ^oC, indicating that the acidic sites in these samples demonstrate weak acidity. After quantification, the total acid amounts for UZSM-5 and Ga- Mo/UZSM-5 catalysts are determined to be 114 and 527 μmol NH_3/g cat, respectively. The modification by Ga and Mo to the UZSM-5 structure significantly increased the number of acid sites, which may improve their catalytic activity in the desulfurization reaction.

3.1 Conclusions

The technical feasibility of marine gas oil and marine diesel oil desulfurization process under a methane environment is verified. The effects of gallium and molybdenum loaded on the homemade UZSM-5 during the desulfurization processes are also investigated by comparison of the sulfur content, liquid yield, total acid number, density, simulated distillation analysis, compositional analysis of the light distillates, and NMR analysis of the liquid products in this study. Catalytic desulfurization under methane is explored using two types of feedstocks, i.e., MGO and MDO, with different compositions. Over 50% sulfur reduction for MGO and MDO with sulfur content around 0.2 wt% is achieved over the Ga-Mo/UZSM-5 catalyst under the CH_4 environment. The participation of CH_4 in the desulfurization results in promoted liquid yield, increased average molecular weight, and density, decreased sulfur content, and TAN compared with its N_2 counterpart.

Chapter Four: Catalytic Methanotreating of Vegetable Oil: A pathway to Second-generation Biodiesel

This chapter is adapted from the following publication:

Yimeng Li, Hao Xu, Zhaofei Li, Shijun Meng, Hua Song. Catalytic methanotreating of vegetable oil: A pathway to Second-generation biodiesel. Fuel 2022; 311: 122504. https://doi.org/10.1016/j.fuel.2021.122504

4.1 Abstract

Vegetable oil is one of the most commonly used feedstocks for the production of biodiesel, while the first-generation biodiesel suffers from the disadvantages of considerable instability and corrosivity. Developing second-generation biodiesel is momentous for the sustainable development of global energy, which overcomes the shortcomings of first-generation biodiesel. The methanotreating of vegetable oil is a potential new route for the production of second-generation biodiesel, which is comprehensively investigated in this study. Throughout the screening of the catalysts, Ga-Ce/TS-1 demonstrates the best overall performance in this methane-incorporated process, leading to 84.23 % of liquid yield, 0.95 % of methane conversion, 72.8 % of oxygen content reduction, and 71% of light hydrocarbon distillates yield. The participation of methane promotes deoxygenation performance, optimizes the composition of paraffinic and olefinic hydrocarbons, as well as suppresses coke formation. The catalytic methanotreating of vegetable oil is confirmed to be a promising pathway to second-generation biodiesel.

4.2 Introduction

The worldwide growth of the economy, development of industrialization, and increase in population are leading to a significantly enhanced demand for fossil fuels. The increasing consumption of fossil fuels not only accelerates the depletion of the reserves but also causes the excessive emission of greenhouse gases and other pollutants such as CO, SO_x, and NO_x. Hence, biodiesel becomes an important part of the global energy structure nowadays because it is renewable and carbon-neutral which benefits the long-term sustainable energy supply and global environment. The first-generation biodiesel, also known as Fatty Acid Methyl Esters (FAME), has been commercialized and mass-produced for years. The common technology for FAME production is catalytic processing of triglycerides (in vegetable oil or fats) with methanol through a

transesterification reaction. Since FAME performs good combustion quality in internal combustion engines and can be easily blended with fossil fuels, the annual production of FAME today is approximately 50 billion liters globally [32]. However, there are some disadvantages of FAME due to its production process and chemical composition. For instance, FAME production generally uses homogeneous base catalysts (e.g. NaOH or KOH) which are non-regenerable, producing a large amount of wastewater as well as low-quality glycerol as a by-product [60]. Moreover, a large amount of oxygen existing in the molecular structure of FAME makes it corrosive as well as thermally and chemically unstable so that it cannot be individually used as automotive fuel [61]. To overcome the drawbacks related to first-generation biodiesel, alternative fuel research is focused on using advanced technologies to produce a more sustainable biofuel known as second-generation biodiesel. Many advanced and popular technologies have been reported such as hydrotreating, catalytic cracking, and catalytic deoxygenation based on the previous studies performed by the researchers [33,62–66]. The oxygen content reduction is dramatic, and the quality of the product oil increases significantly after processing vegetable oils, oleic acid, and FAME under a hydrogen environment. For instance, 97% of oxygen reduction was achieved by hydro-deoxygenation of oleic acid. Meanwhile, the light oil fraction (boiling point < 350 ^{o}C) in the product oil reached 97% of the oil phase products with the $C_{17}H_{36}$ selectivity as high as 85% [66]. Using the catalytic hydro-deoxygenation method to further process FAME results in even better performance. 100% of oxygen reduction and over 96% of $C_{17}H_{36}$ selectivity can be achieved by employing various catalysts [33]. Generally speaking, these technologies use hydrogen gas as an H donor to change the hydrocarbon structures of the feedstock and result in diesel-ranged or gasoline-ranged fuel oil with extremely low oxygen content. However, hydrogen is not naturally available which is normally produced by the steam methane reforming (SMR) process at over 800 ^{o}C and 1.5–3.0 MPa [37,38]. Based on an assessment of hydrogen production, 75% of hydrogen is produced by

SMR globally [36]. Since the SMR process also produces a mass of CO_2 as a by-product, an average of 7 kg CO_2/kg H_2 emitted from SMR facilities has been reported, which will increase the global greenhouse effect. Meanwhile, for the hydrotreatment of second-generation biodiesel production, the required hydrogen pressure is in the range of 4 to 15 MPa which results in a considerable capital and operational cost [31,67]. Thus, directly using methane as the H donor instead of using hydrogen during the production of second-generation biodiesel will significantly reduce the cost, CO_2 emission, and enhance the potential of commercialization.

Using methane, the major component of natural gas, as an alternative hydrogen source has been reported in previous studies such as methanotreating of paraffin [43,45,68,69], olefin [70–72], light fuel oil [52,73], biomass [44,48,49,74], heavy oil [75–77], and bitumen [41,78–81]. Methane has a more stable molecular structure than hydrogen as well as a strong C–H bond with 413 kJ/mol bond energy which makes methane relatively inert to be activated. Therefore, developing catalyst systems that can efficiently break the C–H bond is crucial for methane to participate in the biodiesel production process [73].

In this paper, a commercial catalyst has been initially employed in the methanotreating of canola oil and soybean oil to verify the feasibility of the technique for different vegetable oils. For in-depth study, three types of developed catalysts with Al_2O_3, our homemade low acidity UZSM-5 [73], and TS-1 as the catalyst supports, and gallium and cerium as the active metal components have been used for the methanotreating of canola oil. To evaluate the catalyst performance, gas yield, liquid yield, coke yield were quantified, and simulated distillation analysis, elemental analysis, and ^{1}H NMR analysis were performed for the oil feeds and products. N_2 physisorption, NH_3-TPD, and XRD were conducted for the employed catalysts. Furthermore, the developed catalysts were also used in the canola oil catalytic cracking under a nitrogen environment to

evaluate the effect of methane by comparing the product properties.

4.3 Experimental

4.3.1 Feedstock and chemicals

Food-grade canola oil and soybean oil were purchased from a nearby food market. The gas cylinder containing 10.000% molar of nitrogen and 90.000% molar of methane (Air Liquide) provided the methane as the feed gas with the nitrogen as the internal standard. The gas cylinder containing 99.999% molar of nitrogen (Air Liquide) provided the pure nitrogen feed gas.

4.3.2 Synthesis of catalysts

Al_2O_3 catalyst support with high surface area in 1/8'' pellet was purchased from Alfa Aesar.

UZSM-5 support was synthesized by the following procedures. First, $Al(NO_3)_3 \cdot 9H2O$ (98%, Alfa Aesar) was mixed with 1.0 mol/L tetrapropylammonium hydroxide (TPAOH, Sigma Aldrich) and stirred at room temperature until a clear solution was obtained. Tetraethyl orthosilicate (TEOS, Sigma Aldrich) was then added dropwise to the above solution whilst maintaining stirring. Upon completion of TEOS addition, the solution was left to stir until supersaturation after approximately 1 h. The resulting supersaturated gel was loaded in a Teflon-lined autoclave and treated in a furnace at 170 ^oC for 72 h. Amounts were calculated to obtain a molar ratio of Al_2O_3:80SiO_2:21TPAOH:943H_2O in the gel. After the hydrothermal synthesis, the powder was recovered by centrifugation and washing with deionized (DI) water 3 times. The resultant paste was then heated at 110 ^oC in the oven for 8 h and subsequently calcined in air at a rate of 5 ^oC/min, held at 300 ^oC for 30 min, ramped at the same rate again to 550 ^oC, and held for 4 h. The resultant powder is denoted UZSM- 5 for the ZSM-5 with uniform particle size and compact cylindrical morphology [45].

Titanium silicalite-1 (TS-1) catalyst support was purchased from ACS Material.

The synthesized UZSM-5 support and TS-1 support were extruded to get the shaped pellets with a diameter of 1.0 mm and length of 5.0 mm.

The metal modified Ga-Ce/Al_2O_3, Ga-Ce/UZSM-5, and Ga-Ce/TS-1 catalysts were prepared by wetness impregnation of three types of support with an aqueous solution of cerium nitrate ($Ce(NO_3)_3 \cdot 6H_2O$, Sigma-Aldrich) and gallium nitrate hydrate ($Ga(NO_3)_3 \cdot xH_2O$, Sigma- Aldrich), dried in the oven at 110 ^oC overnight, followed by calcination at 550 ^oC for 4 h in the air after each metal was loaded. The mass percentages of Ce and Ga were 5% and 1%, respectively.

Table 4.1 List of the reactions

Reaction Entry	Catalyst	Feed Gas	Feedstock
1	COM-HZSM-5	CH_4	Canola oil
2	COM-HZSM-5	CH_4	Soybean oil
3	Ga-Ce/Al_2O_3	CH_4	Canola oil
4	Ga-Ce /Al_2O_3	N_2	
5	Ga-Ce /UZSM-5	CH_4	
6	Ga-Ce /UZSM-5	N_2	
7	Ga-Ce /TS-1	CH_4	
8	Ga-Ce /TS-1	N_2	
9	TS-1	CH_4	
10	No catalyst	CH_4	

4.3.3 Catalytic performance evaluation

To make a preliminary attempt for the vegetable oil methanotreating, entries 1 and 2 (Table 4.1) were conducted at 3.0 MPa pressure and a reaction temperature of 400 ^oC using a fixed bed

reactor purchased from SinoGreen Hi-Tech Co. Ltd. The feed gas was a mixed gas (90% CH_4, 10% N_2) with a rate of 100 sccm controlled by a mass flow controller. Canola oil and soybean oil were pumped into the reactor at 0.09 mL/min through a high-pressure metering pump (Eldex Co.) for the first and the second entry, respectively. In both cases, 5 g of an HZSM-5 based commercial catalyst (COM-HZSM-5) obtained from SinoGreen Hi-Tech Co. Ltd., were loaded into the middle part of the reactor, where the void space was filled by two pieces of quartz wool and glass beads (see in Fig. 4.1). The reactor was mounted in a furnace heated to the desired temperature before the reaction began. During the reaction, feedstock passed through the catalyst bed in a down-flow mode. Liquid products were condensed in a stainless-steel condenser at -2 ^oC cooled by a benchtop chiller (PolyScience) and collected after the reaction for further analysis. The outlet gas was firstly depressurized to the atmospheric pressure by a back-pressure regulator then directly introduced into a 490 Micro-GC system (Agilent) for real-time evaluation. Coke was collected after the reaction together with the used catalyst and quantified by a simultaneous thermal analyzer (PerkinElmer STA 6000). The time on stream for both reactions was 6 h.

To further evaluate the performance of another three types of independently developed catalysts including Ga-Ce/Al_2O_3, Ga-Ce/UZSM-5, and Ga-Ce/TS-1, the following six reactions (entries 3–8) were conducted in the same fixed bed reactor system using canola oil as the feedstock. Two reactions were processed under methane and nitrogen environment for each catalyst, and reaction conditions were: temperature = 400 ^oC, pressure = 3.0 MPa, liquid feedstock rate = 0.09 mL/min, feed gas feeding rate = 100 sccm, catalyst load = 2.87 g and time on stream = 3.5 h.

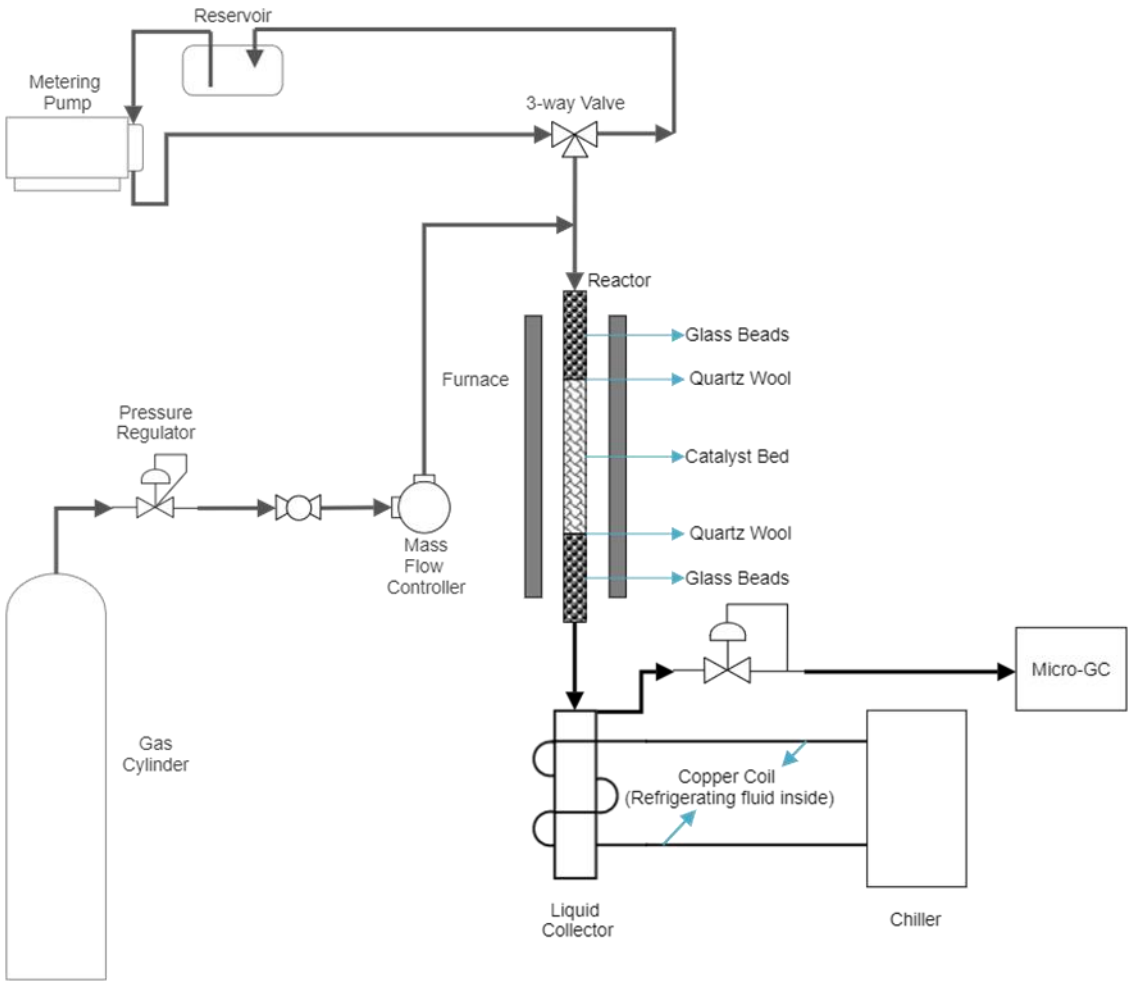

Fig. 4.1 Schematic of the reaction system used for vegetable oil methanotreating

Another two entries (entries 9 and 10) were conducted to identify the catalytic activity of the developed catalysts, especially for Ga-Ce/TS-1. Entry 9 was processed under the methane environment without using any catalyst while entry 10 is also a methanotreating one but over bare TS-1 support. Both entries used the same reaction conditions as entries 3–8.

4.3.4 Characterizations

To determine gas yield and methane conversion, the outlet gas from the reactor system was connected to online gas chromatography (Agilent Micro-GC 490) to obtain the real-time gas composition. The gas yield was calculated using the summation of the average mass of generated

gases divided by the mass of the liquid feedstock pumped into the reactor during the on-stream time. N_2 was regarded as an internal standard to determine the amount of other gaseous species. The methane conversion was acquired by the subtraction of the amount of CH_4 in the inlet gas and the outlet gas divided by the amount of CH_4 in the inlet gas. The liquid yield was the ratio between the mass of the collected liquid product and the mass of consumed feedstock.

Thermogravimetric Analysis (TGA) signals of the spent catalyst were acquired on a simultaneous thermal analyzer (PerkinElmer STA 6000) to calculate the coke yield as well as coke formation rate.

The elemental analysis was achieved by an Elemental Analyzer (Perkin Elmer 2400 Series). C, H, N, and S compositions were directly determined for all oil samples, and the oxygen content of the samples was calculated to meet the mass balance.

Simulated distillation analysis (SDA) of the feedstock and product oil samples was achieved by Agilent 8890 GC System equipped with an analysis software SimDis Expert developed by Separation Systems. The SDA samples were prepared by dissolving 0.1 g of oil samples into 1.5 g CS_2. The boiling point difference among various hydrocarbon species within the oil samples was determined. Liquid nitrogen was used to realize the cryogenic GC analysis from -20 ◦C to 425 ^oC with a ramp rate of 10 ^oC/min. The boiling curves were calibrated using the reference sample SD-SS3E-05 supplied from Separation Systems. The average molecular weight of the oil samples was calculated using these simulated distillation curves.

Proton nuclear magnetic resonance (^1H NMR) analysis was conducted at 9.4 T ($\nu_0(^1H)$ = 400.1 MHz) on a BRUKER AVANCE III 400 spectrometer with a BBFO probe. The NMR samples in the tubes are prepared by mixing 0.1 mg sample with 0.9 mL $CDCl_3$. $CHCl_3$ at 7.28 ppm was set

as the reference for the chemical shifts. 12 kHz of spectral width and a pulse delay of 2 s was used to acquire 64 scans per spectrum.

Ammonia-temperature programmed desorption (NH_3-TPD) was performed on a chemisorption analyzer (Finesorb-3010) to determine the surface acidity of the catalysts. Typically, 0.2 g catalyst powder was put into a U-type quartz tube with quartz wool filled on both ends. Adsorption was conducted by feeding 10% NH_3/He for 30 min (flow rate 25 sccm), followed by purging with He for 30 min (flow rate 30 sccm) to discharge the physisorbed ammonia. Finally, the desorption of ammonia was carried out from 120 ^oC to 600 ^oC with a ramping rate of 10 $^oC\ min^{-1}$ and held at 600 ^oC for 10 min. The amount of desorbed ammonia was quantified by peak integration of the corresponding calibrated thermal conductivity detector (TCD) signal.

X-ray diffraction (XRD) was conducted to examine the crystalline phase compositions of the catalysts on a Rigaku Multiflex diffractometer with Cu Kα irradiation at a voltage of 40 kV and a current of 40 mA in the 2θ range of 5-60^o.

N_2 adsorption-desorption analysis of catalysts was carried out on an ASAP 2020 Plus surface area and porosimeter system (Micromeritics). Degassing of the samples was firstly processed at 350 ^oC for 4 h with a temperature ramping rate of 10 $^oC\ min^{-1}$ and a vacuum level of 20 μmHg. Then the analysis was performed in liquid nitrogen to get a 56-point adsorption-desorption isotherm. The total surface area was calculated by the BET method and the total pore volume was calculated at 0.995 relative pressure. The micropore volume was calculated by the t-plot method.

4.4 Results and discussion

The first two entries of the reactions were conducted under a methane environment using canola oil and soybean oil as feedstock, respectively. Based on the simulated distillation analysis

result (Table 4.2), for both cases, the upgraded product oils have 40 wt% of gasoline fraction and over 34 wt% of diesel fraction. The considerable light oil fraction (< 350 ^{o}C) reveals the relative dramatic hydrocarbon cracking during the reactions which exhibits the potential of this technology to be a promising pathway for second-generation biodiesel production. However, the gas yield of entry 1 and entry 2 are 26.32 wt% and 17.23 wt%, resulting in the corresponding liquid yield as low as 70.08 wt% and 77.48 wt% (Table 4.3). The excessive cracking observed in entries 1 and 2 is possibly due to the large number of acid sites located on the COM-HZSM-5 catalyst. Therefore, to optimize the methanotreating process of canola oil, another three types of catalysts were developed. Al_2O_3, UZSM-5, and TS-1 were selected to be the catalyst support because of their lower acidity compared to HZSM-5. According to the NH_3-TPD results of the various catalyst shown in Fig. 4.2 and Table 4.4, all the developed catalysts have significantly fewer acid sites than COM-HZSM-5. As for metal loading, gallium was selected since it has been verified to be an effective metal in methane activation [54,69,80]. In our previous study, zeolite catalyst doped with cerium can significantly increase its oxygen storage capacity by introducing cerium oxide into the zeolite framework and thus effectively reducing carbon deposition tendency, beneficial for extended catalyst lifetime [82]. Therefore, these two metals were selected as the active components in the developed catalysts.

The mass balance results of entries 3, 5, and 7 (See in Table 4.5) showed that the liquid yield is ranging from 78 wt% to 85 wt% when developed catalysts were used for the methanotreating reactions. Compared to entry 1, the gas yield reduction of these reactions is significant, especially when Ga-Ce/TS-1 was employed. It is noticed that the liquid yield is larger under the nitrogen environment than that under the methane environment for each control group due to the higher gas yield mainly in a form of CO_2 when methane was applied. This phenomenon indicates that methane can promote the intensity of catalytic cracking which may contribute to the greater deoxygenation

performance. On the other hand, the coke formation rate of each methane incorporated reaction is lower than its counterpart process under nitrogen which can be due to the coke inhibition effect of methane confirmed in our previous research [48]. Comparatively speaking, Ga-Ce/TS-1 has the best performance on liquid yield improvement. In addition, it also leads to 0.95% methane conversion during the reaction which is almost doubled compared to Ga-Ce/Al_2O_3 charged one. The significant reduction of coke yield from 6.1% to 4.28% and promotion of methane conversion from 0.15% to 0.95% has been observed by comparing entry 7 and entry 9. It verified that the catalytic activity is enhanced and the coke formation rate is reduced after loading Ga and Ce as the functional metal species on the TS-1 catalyst support.

Table 4.2 Simulated distillation results of entries 1 and 2

Reaction entry	Catalyst	Feed gas	Gasoline range distillate (<200 °C)/%	Diesel range distillate (200 °C-350 °C)/%	Total distillate (<350 °C)/%
/	Feedstock	/	0	0	0
1	COM-HZSM-5	CH_4	40	34	74
2	COM-HZSM-5	CH_4	40	35	75

Table 4.3 Mass balance results of entries 1 and 2

Reaction entry	Catalyst	Feed gas	Gas yield/%	Liquid yield/%	Coke yield/%	Overall yield/%
1	COM-HZSM-5	CH_4	26.32	70.08	2.72	99.12
2	COM-HZSM-5	CH_4	17.23	77.48	3.71	98.42

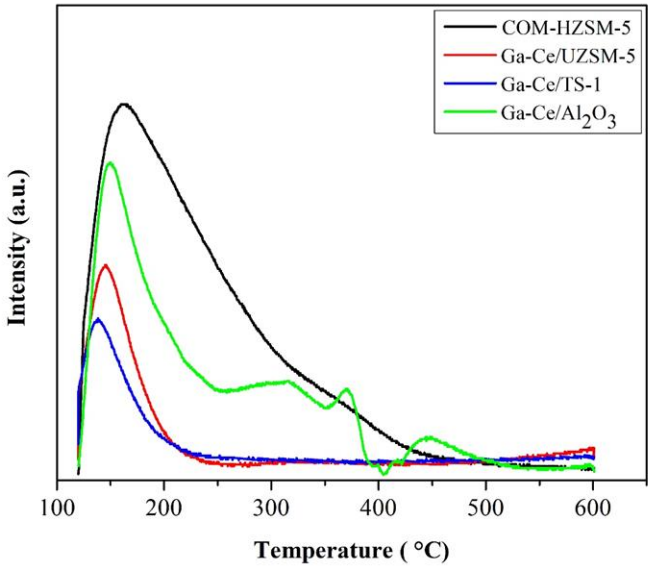

Fig. 4.2 NH_3-TPD curves of various catalysts

Table 4.4 NH_3-TPD results of various catalysts

Catalysts	The densities of different types of acidic sites (μmol NH_3/g)			
	Weak (< 200 ℃)	Medium (200 - 400 ℃)	Strong (> 400 ℃)	Total
COM-HZSM-5	414	155	0	569
Ga-Ce/Al_2O_3	38	5	4	47
Ga-Ce/UZSM-5	35	0	0	35
Ga-Ce/TS-1	25	0	0	25

Table 4.5 Mass balance result of entries 3-10

Entry	Catalyst	Feed gas	Gas yield/%	Liquid yield/%	Coke yield/%	Coke formation rate /h^{-1}	CH_4 conv./%	Overall yield/%
3	Ga-Ce/Al_2O_3	CH_4	14.59	78.53	6.05	0.091	0.54	99.17
4	Ga-Ce/Al_2O_3	N_2	8.76	82.75	6.91	0.110	/	98.42
5	Ga-Ce/UZSM-5	CH_4	11.57	83.80	3.92	0.063	0.61	99.29
6	Ga-Ce/UZSM-5	N_2	7.40	86.90	3.92	0.064	/	98.22
7	Ga-Ce/TS-1	CH_4	10.93	84.23	4.28	0.069	0.95	99.44
8	Ga-Ce/TS-1	N_2	7.08	87.03	4.96	0.080	/	99.07
9	TS-1	CH_4	9.73	83.15	6.10	0.100	0.15	98.98
10	No catalyst	CH_4	3.59	96.41	0	0	0	100

As shown in Fig. 4.3, the SDA curves of product oils in entries 3–8 are significantly shifted to the left compared to the feedstock, resulting in a great reduction of average molecular weight (AMW). The product oil under methane over Ga-Ce/TS-1 catalyst (entry 7) has the lowest AMW of 244.4 g/mol among all the oil products and has 71 wt% of distillates at gasoline range and diesel range in total, larger than 62 wt% and 63 wt % when Ga-Ce/UZSM-5 and Ga-Ce/Al_2O_3 were used respectively (Table 4.6). The observation verified that Ga-Ce/TS-1 has the best performance in converting canola oil into light hydrocarbons. It is worth noting that nearly 100% of light oil fraction (< 350 ^oC) can be achieved by processing oleic acid and FAME through the hydro-deoxygenation method [33,66]. The considerable disparity between methane-assisted deoxygenation and hydro-deoxygenation provides a clear objective for further optimization of the catalysts.

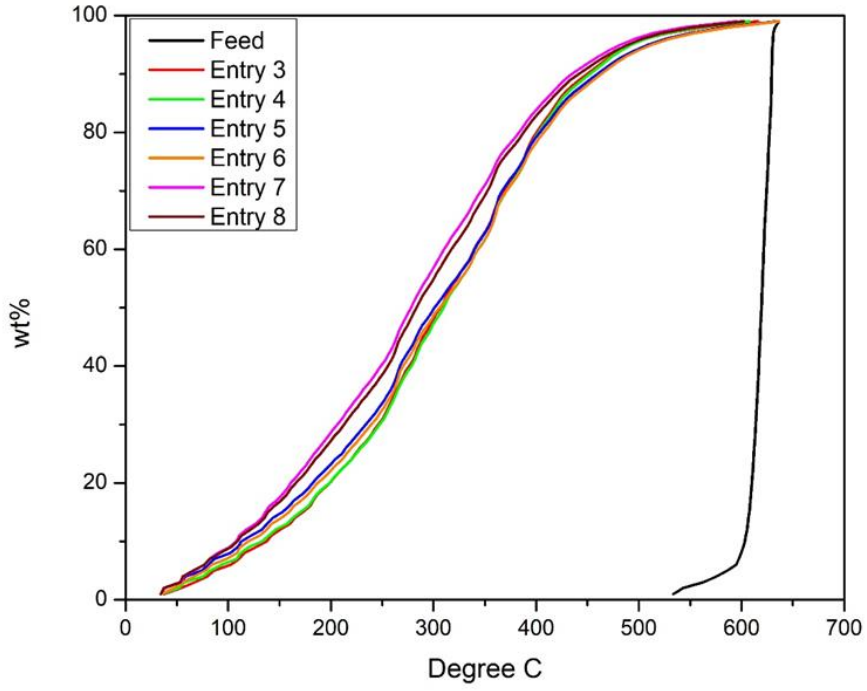

Fig. 4.3 Simulated distillation curves of entries 3-8

Table 4.6 Simulated distillation results of entries 3-8

Reaction entry	Catalyst	Feed gas	Average molecular weight/(g/mol)	Gasoline range distillate (<200 °C)/%	Diesel range distillate (200 °C-350 °C)/%	Total distillate (< 350 °C)
/	Feedstock	/	848.3	0	0	0
3	Ga-Ce/Al_2O_3	CH_4	268.7	20	43	63
4	Ga-Ce/Al_2O_3	N_2	269.5	20	42	62
5	Ga-Ce/UZSM-5	CH_4	269.3	23	39	62
6	Ga-Ce/UZSM-5	N_2	273.5	22	39	61
7	Ga-Ce/TS-1	CH_4	244.4	28	43	71
8	Ga-Ce/TS-1	N_2	250.0	27	42	69

The oxygen content reduction in methanotreating of canola oil is remarkable (Table 4.7). All the products of methane-assisted catalytic reactions have lower oxygen content compared to their counterparts produced in a nitrogen environment. It indicates that methane can promote the breakage of carbon-oxygen bonds. 77.8% oxygen reduction is achieved when Ga-Ce/Al_2O_3 was loaded for the methanotreating process, while Ga-Ce/TS-1 offers 72.8% of oxygen reduction capacity, which is competitive as well. The oxygen reduction in entry 9 is only 7.8%, where no catalyst is employed. It shows that the deoxygenation performance of pure thermal cracking is very limited to under 400 °C. 43.3% oxygen reduction is obtained when bare TS-1 support is applied, much smaller than 72.8% achieved by Ga-Ce/TS-1, which indicates that the deoxygenation performance is remarkably improved after adding Ga and Ce to the TS-1 support. Since lower oxygen content corresponds to lower acidity and corrosivity as well as higher heating value, which are beneficial for the enhanced quality of the products, these results thus provide strong evidence for methanotreating of canola oil being an advanced technology with great potential for second-generation biodiesel production.

Table 4.7 Elemental analysis results of entries 3-10

Reaction entry	Catalyst	Feed gas	Carbon/wt%	Hydrogen /wt%	Oxygen /wt%	Oxygen content reduction /%
/	Feedstock	/	77.64	11.91	10.30	/
3	Ga-Ce/Al_2O_3	CH_4	84.75	13.08	2.17	78.9
4	Ga-Ce/Al_2O_3	N_2	84.51	13.14	2.35	77.2
5	Ga-Ce/UZSM-5	CH_4	83.33	13.04	3.63	64.8
6	Ga-Ce/UZSM-5	N_2	83.32	12.78	3.90	62.1
7	Ga-Ce/TS-1	CH_4	84.16	13.04	2.80	72.8
8	Ga-Ce/TS-1	N_2	83.63	12.77	3.60	65.0
9	TS-1	CH_4	81.60	12.56	5.84	43.3
10	No catalyst	CH_4	78.29	12.21	9.50	7.8

^{1}H NMR analysis was conducted to study the composition of paraffinic, olefinic, and aromatic hydrocarbons within the oil products (Table 4.8). The results show that when the same catalyst was used, the oil samples produced under the methane environment have less olefinic and more aromatic hydrocarbons than the oil samples produced under the nitrogen environment. This observation illustrates that the introduction of methane can improve the oil quality by enhancing the saturation of alkenes as well as aromatization. It is also noticed that the product oil obtained from the methane-assisted reaction when Ga-Ce/TS-1 was applied (entry 7) has the lowest olefin yield (3.52 wt%) among all the oil products, indicating Ga-Ce/TS-1 has a better performance on alkene saturation than Ga-Ce/Al2O3 and Ga-Ce/UZSM-5 which may be due to the observed highest methane conversion when Ga-Ce/TS-1 was employed (Table 4.5). The olefin contents in the products of entries 9 and 10 are significantly higher than other products and feedstock, indicating pure thermal cracking and catalytic cracking over bare TS-1 support produce a considerable amount of unwanted unsaturated hydrocarbons. Loading Ga and Ce as the active

metals on TS-1 can effectively improve the quality of the formed product oil.

Table 4.8 ^{1}H-NMR results of entries 3-10

Reaction entry	Catalyst	Feed gas	Paraffinic/%	Olefinic/%	Aromatic/%
3	Ga-Ce/Al_2O_3	CH_4	92.39	4.44	3.17
4	Ga-Ce/Al_2O_3	N_2	92.24	4.91	2.85
5	Ga-Ce/UZSM-5	CH_4	92.59	4.27	3.15
6	Ga-Ce/UZSM-5	N_2	92.30	4.59	3.11
7	Ga-Ce/TS-1	CH_4	93.12	3.52	3.36
8	Ga-Ce/TS-1	N_2	92.96	3.71	3.33
9	TS-1	CH_4	93.86	6.09	0.05
10	No catalyst	CH_4	93.48	6.30	0.22

XRD analysis was utilized for analyzing fresh and used catalyst samples to obtain information on the catalyst crystal structure. The detected diffraction peaks of used catalysts are quite similar to the corresponding fresh ones, and only slight differences in the intensity of the signals are observed (Fig. 4.4). It demonstrates good stability of the catalyst structures which are not markedly changed after the reaction. The CeO_2 diffraction peaks at 28.55^o ((111) crystal plane) and 33.08^o ((200) crystal plane) in 2Θ can be identified [79]. The intensity of those peaks is decreased after the reactions which might be due to the coke formation on the catalysts' surface. It is also worth mentioning that there are no noticeable diffraction peaks of Ga_2O_3 because loaded Ga only has 1 wt% and Ga species are usually highly dispersed on the surface of the catalysts which has been proved by previous studies [83,84].

N_2 physisorption was carried out to further explore the physical properties of the fresh and used catalysts. The result (Table 4.9) shows that fresh Ga-Ce/Al_2O_3 has almost no micropore and the predominantly mesopores contribute to the largest total pore volume. Fresh Ga-Ce/TS-1 and Ga-

Ce/UZSM-5 are microporous materials whose micropore surface area occupies a large proportion of their total surface area. Ga-Ce/TS-1 has more mesopore volume than Ga-Ce/UZSM-5, and it has an integration of micropores and mesopores (Fig. 4.5), which might be one of the reasons for better performance. By comparing the properties of used catalysts, Ga-Ce/TS-1 has a remarkably larger total surface area, micropore surface area, as well as micropore volume than Ga-Ce/UZSM- 5, proving that Ga-Ce/TS-1 has better tolerance of coke formation than Ga-Ce/UZSM-5, especially for the microporous structures.

Table 4.9 N_2 Physisorption results of the fresh and used catalysts

Catalyst	Feed gas	BET surface area (m^2/g)	Micropore surface area (m^2/g)	External surface area (m^2/g)	Total pore volume (mL/g)	Micropore volume (mL/g)
Ga-Ce/Al_2O_3	/	216	11	206	0.619	0.004
used Ga-Ce/Al_2O_3	CH_4	136	0	156	0.273	0
used Ga-Ce/Al_2O_3	N_2	103	0	130	0.243	0
Ga-Ce/UZSM-5	/	338	185	153	0.314	0.098
used Ga-Ce/UZSM-5	CH_4	19	0	17	0.066	0
used Ga-Ce/UZSM-5	N_2	17	0	21	0.050	0
Ga-Ce/TS-1	/	325	133	192	0.336	0.073
used Ga-Ce/TS-1	CH_4	104	67	37	0.098	0.038
used Ga-Ce/TS-1	N_2	92	63	30	0.089	0.035

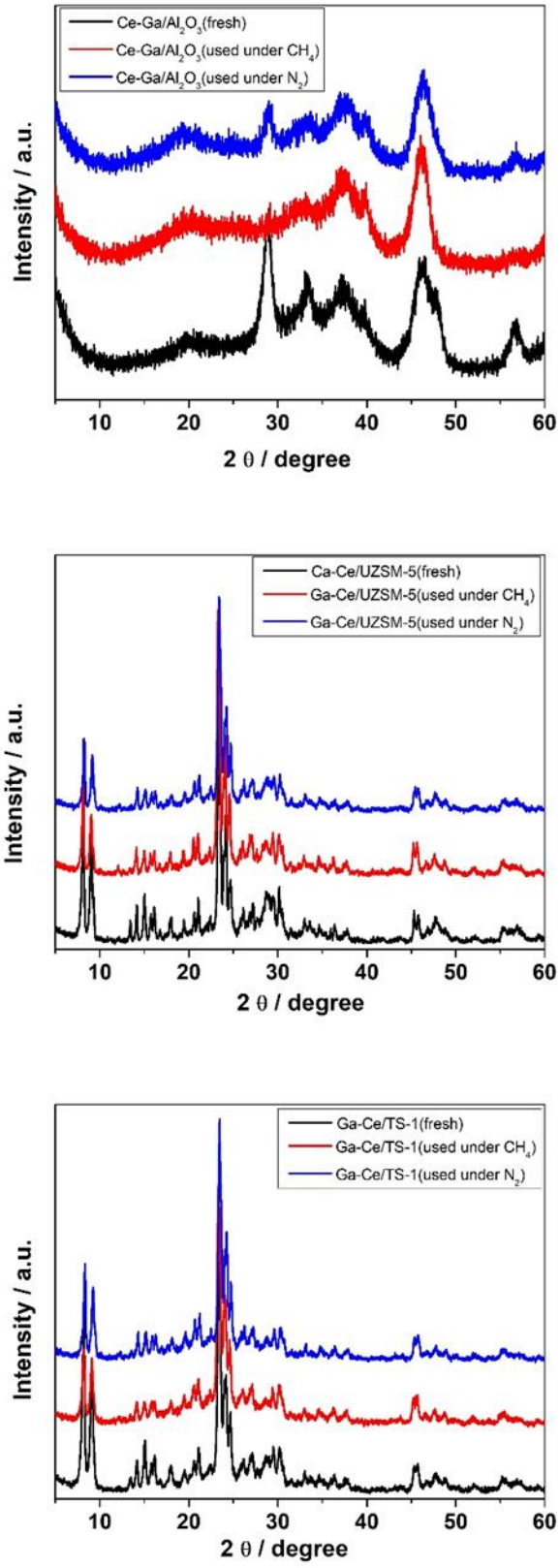

Fig. 4.4 XRD result of the fresh and used catalysts

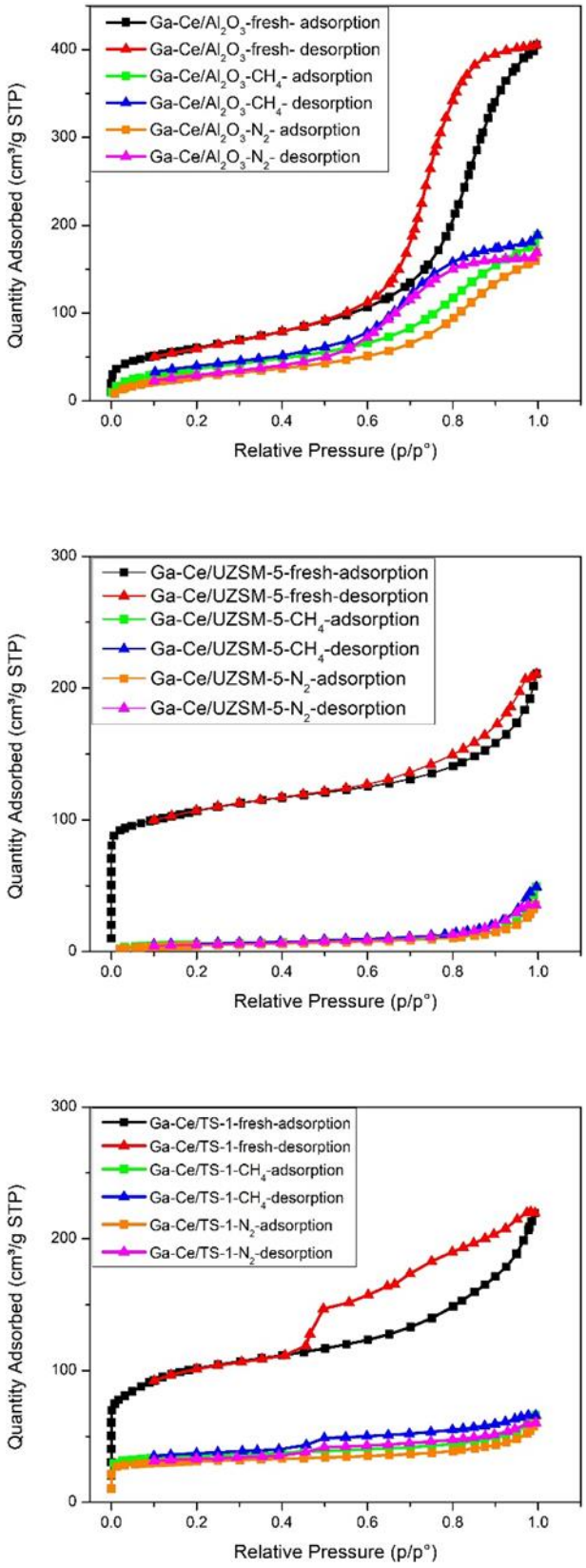

Fig. 4.5 N_2 Physisorption curves of the fresh and used catalysts

4.5 Conclusions

In this study, the technical feasibility of vegetable oil methanotreating is proved. Reaction performances of Ga-Ce/Al_2O_3, Ga-Ce/UZSM-5, and Ga-Ce/TS-1 are investigated by the comparison of the gas yield and coke yield of the reactions, simulated distillation analysis, elemental analysis, and ^1H NMR analysis of the oil products. 84.23 wt% of liquid yield, 72.8% of oxygen content reduction, and 71 wt% of light hydrocarbon fraction (< 350 ^oC) are achieved by Ga-Ce/TS-1 catalyst under the methane environment. Compared with the reactions processed under the nitrogen environment, the introduction of methane in the vegetable oil catalytic cracking process results in lowered coke yield, reduced average molecular weight, promoted oxygen content reduction and decreased yield of olefinic hydrocarbons. According to the deoxygenation performance, there is a certain gap between hydrotreating and methanotreating technologies in the current stage. However, it provides a clear direction for us for the further research and optimization of the catalysts.

Chapter Five: Conclusions and Recommendations

5.1 Conclusions

In this thesis, the technique of catalytic light crude upgrading under a methane environment was systematically explored. Specifically, a series of methane-assisted desulfurization and deoxygenation experiments were evaluated with extensive studies. From the desulfurization perspective, it is conclusive that a combination of Ga-Mo intermetallic particles on UZSM-5 support has a promising performance for sulfur content removal in the presence of methane which achieves a conversion from the MGO and MDO feedstocks with 0.2 wt% of sulfur into the products with less than 0.1 wt% sulfur. From the deoxygenation point of view, a combination of Ga-Ce intermetallic particles on TS-1 support achieves over 70% of oxygen content removal for canola oil under a methane environment. These catalysts and feedstocks were subjected to a continuous fixed-bed flow reactor system to provide ideas of their applicability to industrial-scale production. Methane was compared to nitrogen-controlled experiments and it was seen that methane provides improved liquid yield, improved sulfur content or oxygen content reduction, and reduced coke yield.

When MGO and MDO are employed as the co-feed with methane, the following conclusions were made:

- Ga-Mo presence provided the indispensable acidic sites to promote the sulfur content removal, BTEX yield, as well as methane activation during the reactions.
- Methane presence increased liquid yield and sulfur content reduction compared to the nitrogen environment, possibly due to the incorporation of methane and the liquid feedstocks.

When canola oil is employed as the co-feed with methane, the following conclusions were

made:

- Ga-Ce doped titanium silicate exhibited a promising oxygen removal performance, improved the quality of the product simultaneously which was reflected in a reduction of olefin content and an increment of the light fraction yield, also resulting in a high level of liquid yield, and a low level of coke yield.

- Methane presence promoted oxygen content reduction, decreased the coke yield and the olefin yield compared to the nitrogen environment, possibly due to the incorporation of methane and the liquid feedstock.

- Catalyst crystallinity was maintained throughout the reaction which was confirmed by XRD.

5.2 Recommendations for future work

1. The mechanism of methane-assisted desulfurization and deoxygenation methods should be further investigated. I suggest carrying out model compound studies by processing single species of sulfur-containing substances (such as thiophene, dibenzothiophene, and 4,6-dimethyl dibenzothiophene) or oxygen-containing substance among the constituents of industrial feedstocks. Methane can be monitored through isotopic labeling (i.e $^{13}CH_4$) so that the evolution of methane fractions can be traced during the reactions. Besides, ^{13}C NMR can be utilized to identify the location of ^{13}C species in the liquid product.

2. A long-term process should be conducted to investigate the stability, the change of activity, as well as the regeneration of the catalysts. A larger scaled reactor system may be required for the long-term run. Some technical issues also need to be taken into

consideration including pellet size, pellet shape, possible blockage in pipelines, and possible pressure drops in the reactor system.

3. Further optimization of the reaction conditions should proceed. Adjustable parameters of the reaction conditions including temperature, pressure, space velocity, and types of the reactor system can be properly changed.

4. New catalysts with improved performance will be developed. Support materials with controlled acidity and porosity will be fully explored to suppress the coking and cracking to achieve higher liquid yield and selectivity. Different active metals will be loaded onto the support materials and their loading amount will be optimized. Furthermore, different loading methods will be applied and compared to reach the optimal catalysts for light oil upgrading in the presence of methane.

5. Some new types of feedstocks should be further applied to methane-assisted light crude oil upgrading technologies. For the desulfurization study, high sulfur gasoline, high sulfur diesel, and high sulfur coke naphtha could be used as the liquid feedstocks. For the deoxygenation study, other typical biomass samples such as bio-crude from pyrolysis, oleic acid, and triglycerides also could be applied. Carrying out these in-depth studies will check the general adaptability of the methane-assist desulfurization and deoxygenation approaches, and pave paths for future commercial applications.

References

[1] IMO 2020 - cutting sulphur oxide emissions. Int Marit Organ 2020. https://www.imo.org/en/MediaCentre/HotTopics/Pages/Sulphur-2020.aspx.

[2] P.D. Martyn Lasek, Jack Jordan, Julian Macqueen GR. World Bunker Price. Big Rance Media Inc 2020. Ship&Bunker.com.

[3] Marine Gas Oil (MGO). Marquard & Bahls 2015. https://www.marquard-bahls.com/en/news-info/glossary/detail/term/marine-gasoil-mgo.html.

[4] World Fuel Services. ISO 8217:2017 Tables 1 & 2 Fuel Standard for marine distillate fuels and for marine residual fuels 2019:0–1.

[5] Marine Diesel Oil (MDO） & Intermediate Fuel Oil (IFO). Marquard & Bahls 2015. https://www.marquard-bahls.com/en/news-info/glossary/detail/term/marine-diesel-oil-mdo-intermediate-fuel-oil-ifo.html.

[6] Shafiq I, Shafique S, Akhter P, Yang W, Hussain M. Recent developments in alumina supported hydrodesulfurization catalysts for the production of sulfur-free refinery products: A technical review. Catal Rev 2022;64:1–86. https://doi.org/10.1080/01614940.2020.1780824.

[7] RP S. OGJ FOCUS Refining catalyst market begins to recover in 2010. Oil Gas J 2010;108:40–3.

[8] Fahim MA, Alsahhaf TA, Elkilani A. Chapter 7 - Hydroconversion. In: Fahim MA, Alsahhaf TA, Elkilani ABT-F of PR, editors., Amsterdam: Elsevier; 2010, p. 153–98. https://doi.org/https://doi.org/10.1016/B978-0-444-52785-1.00007-3.

[9] Rana MS, Sámano V, Ancheyta J, Diaz JAI. A review of recent advances in process technologies for upgrading heavy oils and residua. Fuel 2007;86:1216–31. https://doi.org/https://doi.org/10.1016/j.fuel.2006.08.004.

[10] Liu Y, Gao L, Wen L, Zong B. Recent Advances in Heavy Oil Hydroprocessing Technologies. Recent Patents Chem Eng 2009;2:22–36. https://doi.org/http://dx.doi.org/10.2174/2211334710902010022.

[11] Chandran D, Khalid M, Walvekar R, Mubarak NM, Dharaskar S, Wong WY, et al. Deep eutectic solvents for extraction-desulphurization: A review. J Mol Liq 2019;275:312–22. https://doi.org/https://doi.org/10.1016/j.molliq.2018.11.051.

[12] BP. Statistical Review of World Energy globally consistent data on world energy markets. and authoritative publications in the field of energy. BP Energy Outlook 2021 2021;70:8–20.

[13] Przybylski DR. Canola Oil : Physical and Chemical Properties by, n.d.

[14] Srivastava A, Prasad R. Triglycerides-based diesel fuels. Renew Sustain Energy Rev 2000;4:111–33. https://doi.org/10.1016/S1364-0321(99)00013-1.

[15] Lin L, Cunshan Z, Vittayapadung S, Xiangqian S, Mingdong D. Opportunities and challenges for biodiesel fuel. Appl Energy 2011;88:1020–31. https://doi.org/10.1016/j.apenergy.2010.09.029.

[16] Shahid EM, Jamal Y. Production of biodiesel: A technical review. Renew Sustain Energy Rev 2011;15:4732–45. https://doi.org/https://doi.org/10.1016/j.rser.2011.07.079.

[17] Noiroj K, Intarapong P, Luengnaruemitchai A, Jai-In S. A comparative study of KOH/Al2O3 and KOH/NaY catalysts for biodiesel production via transesterification from palm oil. Renew Energy 2009;34:1145–50. https://doi.org/https://doi.org/10.1016/j.renene.2008.06.015.

[18] Kim H-J, Kang B-S, Kim M-J, Park YM, Kim D-K, Lee J-S, et al. Transesterification of vegetable oil to biodiesel using heterogeneous base catalyst. Catal Today 2004;93–95:315–20. https://doi.org/https://doi.org/10.1016/j.cattod.2004.06.007.

[19] Lee J-S, Saka S. Biodiesel production by heterogeneous catalysts and supercritical technologies. Bioresour Technol 2010;101:7191–200. https://doi.org/https://doi.org/10.1016/j.biortech.2010.04.071.

[20] Leung DYC, Wu X, Leung MKH. A review on biodiesel production using catalyzed transesterification.

Appl Energy 2010;87:1083–95. https://doi.org/https://doi.org/10.1016/j.apenergy.2009.10.006.

[21] Wang JX, Chen KT, Huang ST, Chen CC. Application of Li2SiO3 as a heterogeneous catalyst in the production of biodiesel from soybean oil. Chinese Chem Lett 2011;22:1363–6. https://doi.org/https://doi.org/10.1016/j.cclet.2011.05.041.

[22] Dai Y-M, Wu J-S, Chen C-C, Chen K-T. Evaluating the optimum operating parameters on transesterification reaction for biodiesel production over a LiAlO2 catalyst. Chem Eng J 2015;280:370–6. https://doi.org/https://doi.org/10.1016/j.cej.2015.06.045.

[23] Wang J-X, Chen K-T, Wu J-S, Wang P-H, Huang S-T, Chen C-C. Production of biodiesel through transesterification of soybean oil using lithium orthosilicate solid catalyst. Fuel Process Technol 2012;104:167–73. https://doi.org/https://doi.org/10.1016/j.fuproc.2012.05.009.

[24] Dai Y-M, Chen K-T, Chen C-C. Study of the microwave lipid extraction from microalgae for biodiesel production. Chem Eng J 2014;250:267–73. https://doi.org/https://doi.org/10.1016/j.cej.2014.04.031.

[25] Intarapong P, Iangthanarat S, Phanthong P, Luengnaruemitchai A, Jai-In S. Activity and basic properties of KOH/mordenite for transesterification of palm oil. J Energy Chem 2013;22:690–700. https://doi.org/https://doi.org/10.1016/S2095-4956(13)60092-3.

[26] Soetaredjo FE, Ayucitra A, Ismadji S, Maukar AL. KOH/bentonite catalysts for transesterification of palm oil to biodiesel. Appl Clay Sci 2011;53:341–6. https://doi.org/https://doi.org/10.1016/j.clay.2010.12.018.

[27] Mutreja V, Singh S, Ali A. Biodiesel from mutton fat using KOH impregnated MgO as heterogeneous catalysts. Renew Energy 2011;36:2253–8. https://doi.org/https://doi.org/10.1016/j.renene.2011.01.019.

[28] Veljković VB, Banković-Ilić IB, Stamenković OS. Purification of crude biodiesel obtained by heterogeneously-catalyzed transesterification. Renew Sustain Energy Rev 2015;49:500–16. https://doi.org/https://doi.org/10.1016/j.rser.2015.04.097.

[29] Abdullah AZ, Razali N, Mootabadi H, Salamatinia B. Critical technical areas for future improvement in

biodiesel technologies. Environ Res Lett 2007;2. https://doi.org/10.1088/1748-9326/2/3/034001.

[30] Bhuiya MMK, Rasul MG, Khan MMK, Ashwath N, Azad AK, Hazrat MA. Second generation biodiesel: Potential alternative to-edible oil-derived biodiesel. Energy Procedia 2014;61:1969–72. https://doi.org/10.1016/j.egypro.2014.12.054.

[31] Mohammad M, Kandaramath Hari T, Yaakob Z, Chandra Sharma Y, Sopian K. Overview on the production of paraffin based-biofuels via catalytic hydrodeoxygenation. Renew Sustain Energy Rev 2013;22:121–32. https://doi.org/10.1016/j.rser.2013.01.026.

[32] Pattanaik BP, Misra RD. Effect of reaction pathway and operating parameters on the deoxygenation of vegetable oils to produce diesel range hydrocarbon fuels: A review. Renew Sustain Energy Rev 2017;73:545–57. https://doi.org/10.1016/j.rser.2017.01.018.

[33] Li X, Luo X, Jin Y, Li J, Zhang H, Zhang A, et al. Heterogeneous sulfur-free hydrodeoxygenation catalysts for selectively upgrading the renewable bio-oils to second generation biofuels. Renew Sustain Energy Rev 2018;82:3762–97. https://doi.org/10.1016/j.rser.2017.10.091.

[34] Kumar P, Verma D, Sibi MG, Butolia P, Maity SK. Chapter 4 - Hydrodeoxygenation of triglycerides for the production of green diesel: Role of heterogeneous catalysis. In: Maity SK, Gayen K, Bhowmick TKBT-HB, editors., Elsevier; 2022, p. 97–126. https://doi.org/https://doi.org/10.1016/B978-0-12-823306-1.00013-3.

[35] Gosselink RW, Hollak SAW, Chang S-W, van Haveren J, de Jong KP, Bitter JH, et al. Reaction Pathways for the Deoxygenation of Vegetable Oils and Related Model Compounds. ChemSusChem 2013;6:1576–94. https://doi.org/https://doi.org/10.1002/cssc.201300370.

[36] Soltani R, Rosen MA, Dincer I. Assessment of CO2 capture options from various points in steam methane reforming for hydrogen production. Int J Hydrogen Energy 2014;39:20266–75. https://doi.org/10.1016/j.ijhydene.2014.09.161.

[37] Chen Y, Mahecha-Botero A, Lim CJ, Grace JR, Zhang J, Zhao Y, et al. Hydrogen production in a sorption-

enhanced fluidized-bed membrane reactor: Operating parameter investigation. Ind Eng Chem Res 2014;53:6230–42. https://doi.org/10.1021/ie500294k.

[38] Pakhare D, Spivey J. A review of dry (CO2) reforming of methane over noble metal catalysts. Chem Soc Rev 2014;43:7813–37. https://doi.org/10.1039/c3cs60395d.

[39] Song H, Jarvis J, Meng S, Xu H, Li Z, Li W. Methane Activation and Utilization in the Petrochemical and Biofuel Industries. Springer International Publishing; 2021.

[40] Faber J, Ahdour S, Hoen M ´t, Nelissen D, Singh A, Steiner P, et al. Assessment of fuel oil availability-Final Report. Imo 2016; MEPC70/INF:1–186.

[41] He P, Zhao L, Song H. Bitumen partial upgrading over Mo/ZSM-5 under methane environment: Methane participation investigation. Appl Catal B Environ 2017;201:438–50. https://doi.org/10.1016/j.apcatb.2016.08.055.

[42] Kozuch S, Shaik S. How to Conceptualize Catalytic Cycles? The Energetic Span Model. Acc Chem Res 2011;44:101–10. https://doi.org/10.1021/ar1000956.

[43] He P, Jarvis J, Liu L, Song H. The promoting effect of Pt on the co-aromatization of pentane with methane and propane over Zn-Pt/HZSM-5. Fuel 2019;239:946–54. https://doi.org/10.1016/j.fuel.2018.11.079.

[44] He P, Shan W, Xiao Y, Song H. Performance of Zn/ZSM-5 for in Situ Catalytic Upgrading of Pyrolysis Bio-oil by Methane. Top Catal 2016;59:86–93. https://doi.org/10.1007/s11244-015-0508-4.

[45] He P, Chen Y, Jarvis J, Meng S, Liu L, Wen XD, et al. Highly Selective Aromatization of Octane over Pt-Zn/UZSM-5: The Effect of Pt-Zn Interaction and Pt Position. ACS Appl Mater Interfaces 2020;12:28273–87. https://doi.org/10.1021/acsami.0c07039.

[46] Wang A, Austin D, He P, Ha M, Michaelis VK, Liu L, et al. Mechanistic Investigation on Catalytic Deoxygenation of Phenol as a Model Compound of Biocrude Under Methane. ACS Sustain Chem Eng 2019;7:1512–23. https://doi.org/10.1021/acssuschemeng.8b05272.

[47] Wang A, Austin D, Song H. Catalytic Upgrading of Biomass and its Model Compounds for Fuel Production. Curr Org Chem 2019;23:517–29. https://doi.org/http://dx.doi.org/10.2174/1385272823666190416160249.

[48] Wang A, Austin D, He P, Mao X, Zeng H, Song H. Direct catalytic co-conversion of cellulose and methane to renewable petrochemicals. Catal Sci Technol 2018;8:5632–45. https://doi.org/10.1039/c8cy01749b.

[49] Austin D, Wang A, Harrhy JH, Mao X, Zeng H, Song H. Catalytic aromatization of acetone as a model compound for biomass-derived oil under a methane environment. Catal Sci Technol 2018;8:5104–14. https://doi.org/10.1039/c8cy01544a.

[50] Austin D, Wang A, He P, Qian H, Zeng H, Song H. Catalytic valorization of biomass derived glycerol under methane: Effect of catalyst synthesis method. Fuel 2018;216:218–26. https://doi.org/https://doi.org/10.1016/j.fuel.2017.12.018.

[51] Wang A, Austin D, Karmakar A, Bernard GM, Michaelis VK, Yung MM, et al. Methane Upgrading of Acetic Acid as a Model Compound for a Biomass-Derived Liquid over a Modified Zeolite Catalyst. ACS Catal 2017;7:3681–92. https://doi.org/10.1021/acscatal.7b00296.

[52] Jarvis J, Wong A, He P, Li Q, Song H. Catalytic aromatization of naphtha under methane environment: Effect of surface acidity and metal modification of HZSM-5. Fuel 2018;223:211–21. https://doi.org/10.1016/j.fuel.2018.03.045.

[53] Kunlun D, A. CD, Laibao Z, Zhi C, D. RA, N. II, et al. A general synthesis approach for supported bimetallic nanoparticles via surface inorganometallic chemistry. Science (80-) 2018;362:560–4. https://doi.org/10.1126/science.aau4414.

[54] Choudhary VR, Kinage AK, Choudhary T V. Low-temperature nonoxidative activation of methane over H-galloaluminosilicate (MFI) zeolite. Science (80-) 1997;275:1286–8. https://doi.org/10.1126/science.275.5304.1286.

[55] Bedard J, Hong D-Y, Bhan A. CH4 dehydroaromatization on Mo/H–ZSM-5: 1. Effects of co-processing H2 and CH3COOH. J Catal 2013;306:58–67. https://doi.org/https://doi.org/10.1016/j.jcat.2013.06.003.

[56] Ismagilov ZR, Matus E V, Tsikoza LT. Direct conversion of methane on Mo/ZSM-5 catalysts to produce benzene and hydrogen: achievements and perspectives. Energy Environ Sci 2008;1:526–41. https://doi.org/10.1039/B810981H.

[57] Prasad VVDN, Jeong K-E, Chae H-J, Kim C-U, Jeong S-Y. Oxidative desulfurization of 4,6-dimethyl dibenzothiophene and light cycle oil over supported molybdenum oxide catalysts. Catal Commun 2008;9:1966–9. https://doi.org/https://doi.org/10.1016/j.catcom.2008.03.021.

[58] Ali I, Saleh TA. Zeolite-graphene composite as support for molybdenum-based catalysts and their hydrodesulfurization performance. Appl Catal A Gen 2020;598:117542. https://doi.org/https://doi.org/10.1016/j.apcata.2020.117542.

[59] Laredo GC, Pérez-Romo P, Escobar J, Garcia-Gutierrez JL, Vega-Merino PM. Light Cycle Oil Upgrading to Benzene, Toluene, and Xylenes by Hydrocracking: Studies Using Model Mixtures. Ind Eng Chem Res 2017;56:10939–48. https://doi.org/10.1021/acs.iecr.7b02827.

[60] Saba T, Estephane J, El Khoury B, El Khoury M, Khazma M, El Zakhem H, et al. Biodiesel production from refined sunflower vegetable oil over KOH/ZSM5 catalysts. Renew Energy 2016;90:301–6. https://doi.org/10.1016/j.renene.2016.01.009.

[61] Bayat A, Sadrameli SM. Conversion of canola oil and canola oil methyl ester (CME) to green aromatics over a HZSM-5 catalyst: A comparative study. RSC Adv 2015;5:28360–8. https://doi.org/10.1039/c5ra01691f.

[62] Kalnes T, Shonnard DR, Marker T. INTERNATIONAL JOURNAL OF CHEMICAL REACTOR ENGINEERING Green Diesel: A Second Generation Biofuel Green Diesel: A Second Generation Biofuel 2007;5.

[63] Li S, Wang Y, Dong S, Chen Y, Cao F, Chai F, et al. Biodiesel production from Eruca Sativa Gars vegetable oil and motor, emissions properties. Renew Energy 2009;34:1871–6. https://doi.org/10.1016/j.renene.2008.12.020.

[64] Snåre M, Mäki-Arvela P, Simakova IL, Myllyoja J, Murzin DY. Overview of catalytic methods for production of next generation biodiesel from natural oils and fats. Russ J Phys Chem B 2009;3:1035–43. https://doi.org/10.1134/S1990793109070021.

[65] Lestari S, Mäki-Arvela P, Beltramini J, Lu GQM, Murzin DY. Transforming triglycerides and fatty acids into biofuels. ChemSusChem 2009;2:1109–19. https://doi.org/10.1002/cssc.200900107.

[66] Zhang Z, Bi G, Zhang H, Zhang A, Li X, Xie J. Highly active and selective hydrodeoxygenation of oleic acid to second generation bio-diesel over SiO2-supported CoxNi1−xP catalysts. Fuel 2019;247:26–35. https://doi.org/10.1016/j.fuel.2019.03.021.

[67] Šimáček P, Kubička D, Šebor G, Pospíšil M. Fuel properties of hydroprocessed rapeseed oil. Fuel 2010;89:611–5. https://doi.org/10.1016/j.fuel.2009.09.017.

[68] Li Q, He P, Jarvis J, Bhattacharya A, Mao X, Wang A, et al. Catalytic co-aromatization of methane and heptane as an alkane model compound over Zn-Ga/ZSM-5: A mechanistic study. Appl Catal B Environ 2018;236:13–24. https://doi.org/10.1016/j.apcatb.2018.05.006.

[69] Li Q, Zhang F, Jarvis J, He P, Yung MM, Wang A, et al. Investigation on the light alkanes aromatization over Zn and Ga modified HZSM-5 catalysts in the presence of methane. Fuel 2018;219:331–9. https://doi.org/10.1016/j.fuel.2018.01.104.

[70] He P, Wen Y, Jarvis J, Gatip R, Austin D, Song H. Selective Participation of Methane in Olefin Upgrading over Pd/ZSM-5 and Ir/ZSM-5: Investigation using Deuterium Enriched Methane. ChemistrySelect 2017;2:252–6. https://doi.org/10.1002/slct.201601625.

[71] He P, Jarvis J, Meng S, Wang A, Kou S, Gatip R, et al. Co-aromatization of methane with olefins: The role

of inner pore and external surface catalytic sites. Appl Catal B Environ 2018;234:234–46. https://doi.org/10.1016/j.apcatb.2018.04.034.

[72] Lou Y, He P, Zhao L, Cheng W, Song H. Olefin Upgrading over Ir/ZSM-5 catalysts under methane environment. Appl Catal B Environ 2017;201:278–89. https://doi.org/10.1016/j.apcatb.2016.08.047.

[73] Li Y, He P, Li Z, Xu H, Jarvis J, Meng S, et al. Catalytic desulfurization of marine gas oil and marine diesel oil under methane environment. Fuel 2021;289:119864. https://doi.org/10.1016/j.fuel.2020.119864.

[74] He P, Song H. Catalytic conversion of biomass by natural gas for oil quality upgrading. Ind Eng Chem Res 2014;53:15862–70. https://doi.org/10.1021/ie502272j.

[75] Guo A, Wu C, He P, Luan Y, Zhao L, Shan W, et al. Low-temperature and low-pressure non-oxidative activation of methane for upgrading heavy oil. Catal Sci Technol 2016;6:1201–13. https://doi.org/10.1039/c5cy00947b.

[76] He P, Meng S, Song Y, Liu B, Song H. Heavy oil catalytic upgrading under methane environment: A small pilot plant evaluation. Fuel 2019;258:116161. https://doi.org/https://doi.org/10.1016/j.fuel.2019.116161.

[77] Li Z, Li Y, Xu H, Jarvis J, Meng S, Song H. Effect of methane presence on catalytic heavy oil partial upgrading. Fuel 2021;297:120733. https://doi.org/10.1016/j.fuel.2021.120733.

[78] Xu H, Li Z, Pryde RL, Meng S, Li Y, Song H. Participation of methane in an economically and environmentally favorable catalytic asphaltene upgrading process. Chem Commun 2020;56:5492–5. https://doi.org/10.1039/d0cc01736a.

[79] Zhao L, He P, Jarvis J, Song H. Catalytic Bitumen Partial Upgrading under Methane Environment over Ag-Mo-Ce/ZSM-5 Catalyst and Mechanistic Study Using N-Butylbenzene as Model Compound. Energy and Fuels 2016;30:10330–40. https://doi.org/10.1021/acs.energyfuels.6b02374.

[80] He P, Luan Y, Zhao L, Cheng W, Wu C, Chen S, et al. Catalytic bitumen partial upgrading over Ag-Ga/ZSM-5 under methane environment. Fuel Process Technol 2017;156:290–7.

https://doi.org/https://doi.org/10.1016/j.fuproc.2016.09.010.

[81] Xu H, Li Z, Li Y, Song H. Catalytic asphaltene upgrading under methane environment: Solvent effect and its interaction with oil components. Fuel 2021;291:120157. https://doi.org/10.1016/j.fuel.2021.120157.

[82] Zhao L, He P, Jarvis J, Song H. Catalytic Bitumen Partial Upgrading under Methane Environment over Ag-Mo-Ce/ZSM-5 Catalyst and Mechanistic Study Using N-Butylbenzene as Model Compound. Energy & Fuels 2016;30:10330–40. https://doi.org/10.1021/acs.energyfuels.6b02374.

[83] Wannapakdee W, Wattanakit C, Paluka V, Yutthalekha T, Limtrakul J. One-pot synthesis of novel hierarchical bifunctional Ga/HZSM-5 nanosheets for propane aromatization. RSC Adv 2016;6:2875–81. https://doi.org/10.1039/c5ra22707k.

[84] Lee BJ, Hur YG, Kim DH, Lee SH, Lee KY. Non-oxidative aromatization and ethylene formation over Ga/HZSM-5 catalysts using a mixed feed of methane and ethane. Fuel 2019;253:449–59. https://doi.org/10.1016/j.fuel.2019.05.014.

Appendix

This Agreement between Mr. Yimeng Li ("You") and Elsevier ("Elsevier") consists of your license details and the terms and conditions provided by Elsevier and Copyright Clearance Center.

License Number	5257380714931
License date	Feb 27, 2022
Licensed Content Publisher	Elsevier
Licensed Content Publication	Elsevier Books
Licensed Content Title	Hydrocarbon Biorefinery
Licensed Content Author	Pankaj Kumar,Deepak Verma,Malayil Gopalan Sibi,Paresh Butolia,Sunil K. Maity
Licensed Content Date	Jan 1, 2022
Licensed Content Pages	30
Type of Use	reuse in a thesis/dissertation
Portion	figures/tables/illustrations
Number of figures/tables/illustrations	1
Format	electronic
Are you the author of this Elsevier chapter?	No
Will you be translating?	No
Title	Catalytic Light Crude Upgrading under Methane Environment
Institution name	University of Calgary
Expected presentation date	May 2022
Order reference number	20220227-015
Portions	figure 4.12

This Agreement between Mr. Yimeng Li ("You") and Elsevier ("Elsevier") consists of your license details and the terms and conditions provided by Elsevier and Copyright Clearance Center.

License Number	5257380592241
License date	Feb 27, 2022
Licensed Content Publisher	Elsevier
Licensed Content Publication	Elsevier Books
Licensed Content Title	Hydrocarbon Biorefinery
Licensed Content Author	Pankaj Kumar,Deepak Verma,Malayil Gopalan Sibi,Paresh Butolia,Sunil K. Maity
Licensed Content Date	Jan 1, 2022
Licensed Content Pages	30
Type of Use	reuse in a thesis/dissertation
Portion	figures/tables/illustrations
Number of figures/tables/illustrations	1
Format	electronic
Are you the author of this Elsevier chapter?	No
Will you be translating?	No
Title	Catalytic Light Crude Upgrading under Methane Environment
Institution name	University of Calgary
Expected presentation date	May 2022
Order reference number	20220227-014
Portions	figure 4.2

This Agreement between Mr. Yimeng Li ("You") and Elsevier ("Elsevier") consists of your license details and the terms and conditions provided by Elsevier and Copyright Clearance Center.

License Number	5257380460512
License date	Feb 27, 2022
Licensed Content Publisher	Elsevier
Licensed Content Publication	Renewable and Sustainable Energy Reviews
Licensed Content Title	Production of biodiesel: A technical review
Licensed Content Author	Ejaz M. Shahid,Younis Jamal
Licensed Content Date	Dec 1, 2011
Licensed Content Volume	15
Licensed Content Issue	9
Licensed Content Pages	14
Type of Use	reuse in a thesis/dissertation
Portion	figures/tables/illustrations
Number of figures/tables/illustrations	1
Format	electronic
Are you the author of this Elsevier article?	No
Will you be translating?	No
Title	Catalytic Light Crude Upgrading under Methane Environment
Institution name	University of Calgary
Expected presentation date	May 2022
Order reference number	20220227-013
Portions	figure 1

This Agreement between Mr. Yimeng Li ("You") and Elsevier ("Elsevier") consists of your license details and the terms and conditions provided by Elsevier and Copyright Clearance Center.

License Number	5257380287297
License date	Feb 27, 2022
Licensed Content Publisher	Elsevier
Licensed Content Publication	Applied Energy
Licensed Content Title	Opportunities and challenges for biodiesel fuel
Licensed Content Author	Lin Lin,Zhou Cunshan,Saritporn Vittayapadung,Shen Xiangqian,Dong Mingdong
Licensed Content Date	Apr 1, 2011
Licensed Content Volume	88
Licensed Content Issue	4
Licensed Content Pages	12
Type of Use	reuse in a thesis/dissertation
Portion	figures/tables/illustrations
Number of figures/tables/illustrations	1
Format	electronic
Are you the author of this Elsevier article?	No
Will you be translating?	No
Title	Catalytic Light Crude Upgrading under Methane Environment
Institution name	University of Calgary
Expected presentation date	May 2022
Order reference number	20220227
Portions	Figure 2